Development of antigen-decorated norovirus-like particles for vaccine applications

Vili Lampinen

Master's thesis

University of Tampere

Faculty of Medicine and Life Sciences

April 2018

Pro Gradu -tutkielma

Paikka:	TAMPEREEN YLIOPISTO Lääketieteen ja biotieteiden tiedekunta (MED)
Tekijä:	LAMPINEN, VILI PETTERI
Otsikko:	Norovirusten kaltaisten partikkelien kehittäminen rokotesovelluksia varten
Sivumäärä:	65
Ohjaaja:	FT Minna Hankaniemi
Tarkastajat:	Apulaisprofessori Vesa Hytönen ja FT Suvi Heinimäki
Päiväys:	Huhtikuu 2018

Tiivistelmä

Nykyisissä influenssarokotteissa on vakavia puutteita, minkä vuoksi lukemattoman suuri määrä ihmisiä sairastuu ja yli 200 000 kuolee kausi-influenssan takia vuosittain. Tässä tutkielmassa pyrittiin luomaan rokoteprototyyppi, jonka tuotanto olisi edullista ja joka tuottaisi pitkäkestoisen immuunivasteen useita influenssakantoja vastaan. Käyttämällä stabiileja ja helposti tuotettavia noroviruksen kaltaisia partikkeleita rokotealustana, uusien rokotetyyppien kehittäminen on merkittävästi nopeampaa. Partikkelit voidaan päällystää joustavasti ja pysyvästi konservoituneilla antigeeneillä hyödyntämällä joko avidiini-biotiini- tai SpyCatcher/SpyTag-teknologiaa.

Konservoitu fragmentti influenssan matrix-2- ja hemagglutiniiniproteiineista yhdistettiin geneettisesti SpyCatcher-proteiiniin tai avidiiniin ja tuotettiin *E. colissa*. Avidiiniin yhdistettyjä antigeenejä ei onnistuttu tuottamaan, mutta SpyCatcher-antigeenifuusioproteiinit tuottuivat voimakkaasti BL21 Star *E. colissa*. Prosessioptimoinnin ja affiniteettikromatografiapuhdistuksen jälkeen proteiinit olivat >95 % puhtaita. Saanto oli 34 mg/L matrix-2- ja 27 mg/L hemagglutiniinifuusioproteiinille. SpyTag yhdistettiin geneettisesti noroviruksen kaltaisen partikkelin pinnalle, mikä mahdollistaa sen pinnoituksen SpyCatcher-proteiinilla. Vaihtoehtoisesti partikkeli päällystettiin AviTagilla, mikä mahdollistaa pinnoituksen avidiinilla. Noroviruspartikkelit tuotettiin Hi5-hyönteissolulinjassa ja puhdistettiin sentrifugoimalla ne ensin 30 % sakkaroosikerroksen läpi ja sitten kationinvaihtokromatografialla. Lopputuotteena saatiin >95 % puhtaita partikkeleita noin 11 mg/L saannolla.

SpyTagilla varustettuja noroviruspartikkeleita sekoitettiin SpyCatcher-antigeenien kanssa puskuriliuoksessa. SDS-PAGE -analyysi osoitti, että nämä komponentit olivat muodostaneet kovalenttisen sidoksen keskenään. Dynaamisella valonsironnalla varmistettiin, että pinnoitetut partikkelit olivat monodispergoituja ja hydrodynaamiselta halkaisijaltaan noin 50 nm, joka vastaa aiempia noroviruksen kaltaisten partikkelien tutkimuksia. Lisäksi todistettiin Western blot-analyysillä, että avidiini sitoutuu AviTag-noroviruspartikkeleihin. Jatkotutkimuksissa näitä rokotteita voidaan käyttää prekliinisiin eläinkokeisiin.

Avainsanat: norovirus, influenssa, viruksenkaltainen partikkeli, VLP, rokote, proteiiniteknologia, biokonjugaatio, SpyCatcher, avidiini

Master's thesis

Place:	University of Tampere Faculty of Medicine and Life Sciences (MED)
Author:	LAMPINEN, VILI PETTERI
Title:	Development of antigen-decorated norovirus-like particles for vaccine applications
Pages:	65
Supervisor:	Minna Hankaniemi, PhD
Reviewers:	Associate professor Vesa Hytönen and Suvi Heinimäki, PhD
Date:	April 2018

Abstract

Due to limitations in current influenza vaccines, an innumerable number of people are taken to bed and over 200,000 lives are lost yearly to seasonal influenza. This thesis work aimed to create a prototype vaccine that would be inexpensive to manufacture and that could generate a powerful immune response, effective against multiple influenza strains for several years, or even decades. Using the robust and easy-to-produce norovirus-like particle as a vaccine platform can reduce the generation time of new vaccines. The particles can be conveniently decorated with conserved antigens using the high-affinity avidin-biotin bond or the isopeptide-bond-forming SpyCatcher/SpyTag pair.

Conserved fragments of the influenza matrix-2 and hemagglutinin protein were genetically fused to SpyCatcher or a selected type of avidin and expressed in *E. coli*. Avidin-fused antigens could not be extracted in a useful form, but the SpyCatcher-antigen fusion proteins were expressed efficiently in BL21 Star *E. coli*. After process optimization, respective yields of 34 and 27 mg/L of SpyCatcher-fused matrix-2 and hemagglutinin fragments were obtained. The yields were estimated for the >95% pure end products of single-step affinity chromatography purification processes. SpyTag or AviTag were genetically fused to norovirus-like particles to allow for their decoration with SpyCatcher or avidin, respectively. The particles were produced in the Hi5 insect cell line and purified with 30% sucrose cushion pelleting, followed by cation exchange chromatography. This resulted in over 95% pure norovirus-like particles with an approximate yield of 11 mg/L.

SpyTagged norovirus-like particles and SpyCatcher-antigens were mixed together. SDS-PAGE analysis showed that the components had covalently conjugated and dynamic light scattering studies confirmed monodisperse, decorated particles with hydrodynamic diameters of around 50 nm, which is similar to previously studied norovirus-like particles. In addition, Western blotting showed that the AviTagged norovirus-like particles are biotinylated and that avidin can bind them. The antigen-decorated virus-like particles are ready for use in pre-clinical animal experiments.

Keywords: norovirus, influenza, virus-like particle, VLP, vaccine, protein technology, bioconjugation, SpyCatcher, avidin

Preface

This thesis work was done in the Protein Dynamics research group under the Faculty of Medicine and Life Sciences of the University of Tampere.

I would like to use this opportunity to thank associate professor Vesa Hytönen for introducing me to the world of protein engineering during my university studies and for giving me the opportunity to finalize (this part of) them researching this exciting new technology in the field. I would also like to thank my supervisor Minna Hankaniemi, PhD, for "consulting" me through the thesis project and docent Olli Laitinen for the feedback, article tips and all other guidance given. Vesna Blazevic, PhD, deserves my gratitude for the support she provided for this project.

Additionally, I thank Niila Saarinen, MSc, for the help in planning the bacterial expression trials, the useful technical and writing hints and for the all the bad humor. Álvaro Garcés Cardona also provided a lot of help in optimizing the bacterial production processes in this project, and I feel we both learned a lot together. The Protein Dynamics group as a whole provided me with support always when needed and welcomed me warmly to this wonderful community. Especially the irreplaceable lab technicians of the group, Niklas Kähkönen and Ulla Kiiskinen, deserve my thanks for the extensive technical support and teaching that I received during this thesis work. Finally, I would like to thank my fellow students, friends and family for providing me with much-needed distraction, new perspectives and even the occasional study-related discussions during my Bachelor's and Master's studies.

Tampere, April 2018

Vili Lampinen

1 Contents

1 Contents iv

2 Introduction 1

3 Literature review 3

3.1 Influenza 3

3.2 Avidins 9

3.3 SpyCatcher/SpyTag 11

3.4 Vaccines based on virus-like particles 12

4 Aims of the study 15

5 Materials and Methods 17

5.1 Antigen production 17

5.2 Norovirus-like particle production 21

5.3 SpyCatcher/SpyTag conjugation 25

5.4 Avidin binding studies with AviTagged noro-VLP 25

5.5 Main methods and their principles 26

6 Results 32

6.1 Production of antigens 32

6.2 Production of virus-like particles 39

6.3 SpyCatcher/SpyTag conjugation 44

6.4 Avidin binding studies with AviTagged norovirus-like particles 45

7 Discussion 47

8 Conclusions 53

9 References 54

10 Appendix: Amino acid sequences of designed proteins 59

Abbreviations

Amp	Ampicillin
Avi-noro-VLP	AviTagged norovirus-like particle
BSA	Bovine serum albumin
CNCA	Charge-neutralized chimeric avidin
cRNA	A full-length complementary copy of influenza RNA
DLS	Dynamic light scattering
dpi	Days post infection
FBS	Fetal bovine serum
Gluc	D-glucose
H1F	Protein derived from H1N1 influenza HA protein, with Foldon trimerization domain
HA	Influenza hemagglutinin protein
IMAC	Immobilized metal affinity chromatography
IPTG	Isopropyl β-D-1-thiogalactopyranoside (an allolactose analog)
LB	Lysogeny broth, bacterial growth medium
M1	Influenza matrix-1 protein
M2e	Ectodomain of influenza matrix-2 protein
MHC	Major histocompatibility complex
MOI	Multiplicity of infection
NA	Influenza neuraminidase protein
noro-VLP	Norovirus-like particle
NP	Influenza nucleocapsid protein
NS	Influenza non-stuctured protein
OD	Optical density
ORF	Open reading frame
PBS	Phosphate-buffered saline
PEG	Polyethylene glycol
RNP	Ribonucleoprotein, RNA bound to proteins
SDS-PAGE	Sodium dodecyl sulfate polyacrylamide gel electrophoresis
Spy-noro-VLP	SpyTagged norovirus-like particle
TBS(-T)	Tris-buffered saline (with Tween 20)
TE-buffer	Tris-EDTA(ethylenediaminetetra-acetic acid) buffer
WB	Western blotting
VLP	Virus-like particle

2 Introduction

Influenza imposes a considerable disease burden worldwide and it constitutes a constant threat to public health. On a global scale, influenza infections cause 250,000–500,000 deaths every year [1], while emerging pandemic strains threaten the lives of millions. In addition, the enormous amount of non-lethal infections causes substantial costs for the society in terms of lost working days on sick leave and public medical expenses. Vaccination remains the most effective strategy in fighting influenza[1,2], but because of the rapid evolution of influenza virus surface proteins, influenza vaccinations need to be renewed annually, and yet there are years when the vaccine lacks effectiveness.

Traditionally, influenza vaccines are inactivated whole or disrupted ("split") viruses that are produced in chicken eggs [2,3]. This technology has been in use since the first influenza vaccine was approved for civil use in 1946 [4]. Conventional influenza vaccines can generate a strong antibody response against a narrow target group of influenza strains. As the generation of a new vaccine takes at least 6 months with this technology [5], the World Health Organization, which coordinates vaccine manufacture, must give recommendations on which strains to include in the next year's vaccine over 6 months beforehand [2]. The recommendations are based on following the development of current circulating strains and predicting their evolution and future transmissibility.

Prediction of the antigenic characteristics of next year's dominant strains is difficult and sometimes mistakes are made, potentially with devastating results. An example of this is the global H1N1 pandemic of 2009, "the swine flu", which unexpectedly went through genetic shift and transformed to resemble the 1918 H1N1 strain ("the Spanish flu") more than any other known strain in the preceding 90-year period [6,7]. The new virus quickly spread all over the globe to replace the previous circulating H1N1 strain, infecting over 22 million people before a vaccine could be administered extensively [8,9]. Fortunately, the virus infections were not nearly as dangerous as with the 1918 pandemic, resembling more an ordinary seasonal influenza in their symptoms.

Conventional vaccines tend to lack long-term protection and cross-protection against multiple types of viruses. Their production requires very specialized expression systems,

which makes them time-consuming and expensive to manufacture. Another drawback of the traditional way of manufacturing influenza vaccines is that the viruses may obtain mutations while grown in eggs. These mutations can differentiate the viruses in the vaccines from their intended forms, and thus weaken the effect of the vaccines [10]. This is particularly problematic with the quickly mutating H3N2 strains. Consequently, there is a clear need to develop less expensive manufacturing systems for modern vaccine formulae to obtain safer and more effective vaccines.

To develop better influenza vaccines, we used the ectodomain of the matrix-2 ion channel protein (M2e) and a minimized stem-fragment of the hemagglutinin (HA) glycoprotein as target influenza antigens. Both protein fragments are highly conserved across different influenza strains from a large time span [11]. A vaccine that can create antibodies against these conserved influenza protein sequences could potentially work as a universal vaccine, ideally protecting against pathogenic influenza types without annual renewal [6,12]. Generating such antibodies has proven impossible when vaccinating with natural viruses, because both conserved regions are concealed underneath the highly variable regions in the immunodominant head domains of HA and neuraminidase (NA) proteins. When fused to a virus-like particle (VLP), the conserved antigen fragments could be displayed in an immunogenic way without the interfering proteins [1].

The simplest way to produce these VLP-bound antigens would be to just genetically fuse them to a virus capsid protein capable of forming the VLP. However, as this approach often hinders VLP assembly, it requires laborious and time-intensive planning and optimization individually for each antigen tested [13]. Therefore, it is not necessarily any easier than conventional vaccine generation processes. To really create a more efficient method of manufacturing vaccines, we chose a modular approach. Here, a single VLP product is used as a platform to which multiple different kinds of modified antigens can be attached easily with the practical method of mixing in solution. Centralized manufacture of the modifiable vaccine platform is cost-efficient and allows formation of large stockpiles of it in case of emerging pandemics. Generating each new vaccine in an identical way should also speed up the regulatory process significantly compared to a different vaccine formula for each generation or kind of pathogen [14].

3 Literature review

3.1 Influenza

3.1.1 Overview and life cycle

Influenza viruses A, B, C and D are all members of the *Orthomyxoviridae* family [3]. The genome of the enveloped virion is assembled into eight (or seven in the case of influenza C) distinct segments of single-stranded, negative-sense RNA [2,3]. The virions are usually spherical and 100–200 nm in diameter, but for some strains, filamentous forms are known [3,9]. These filaments are similar in breadth to the spherical forms but can reach lengths of 20,000 nm. Viruses from genera A and B are the most harmful to humans and cause seasonal epidemics on a regular basis [15]. Influenza C also causes some infections with minor symptoms in humans from time to time, but the D genus has not been observed infecting humans. It is primarily a cattle pathogen.

Membranes derived from the host cell envelop influenza virions. Some 500 large glycoproteins protrude from the lipid membrane of an average virion, about 80% of which are HA, the rest NA [3] (Figure 1). Additionally, a few matrix-2 (M2) proteins penetrate the membrane with their small ectodomains. Inside the membrane lies the protein capsid of the virion, which is composed of the matrix-1 (M1) protein. The RNA genome of influenza is packed together with the nucleocapsid protein (NP) and the viral polymerases PA, PB1 and PB2 into ribonucleoprotein (RNP) that forms the core of a virion [9]. M1 links RNP to the viral capsid.

The first step in influenza infection on the cellular level is the binding of sialic acids on cell surface proteins with the HA head domain [9]. The term “influenza receptor” is commonly used in literature, but it can be misleading since it suggests an active role to this not-so-definite group of proteins. In principle, any cell surface protein that contains the right kinds of post-translational modifications can facilitate HA binding, and thus act as a receptor for the virus. The species specificity of different influenza strains is in part explained by the binding preferences of their HA protein [3]. For example, HA from avian influenza binds sialic acids that are linked to galactose via an α-2,3-glycosidic bond best, while human influenza HA prefers sialic acids with α-2,6-glycosidic bonds [7].

These kinds of sialic acids are most common in endothelial cells of the respiratory track, which is related to the tissue tropism of influenza [16]. Hemagglutinin also binds sialic acids on the surface of erythrocytes, causing their agglutination; hence the name of the protein [17].

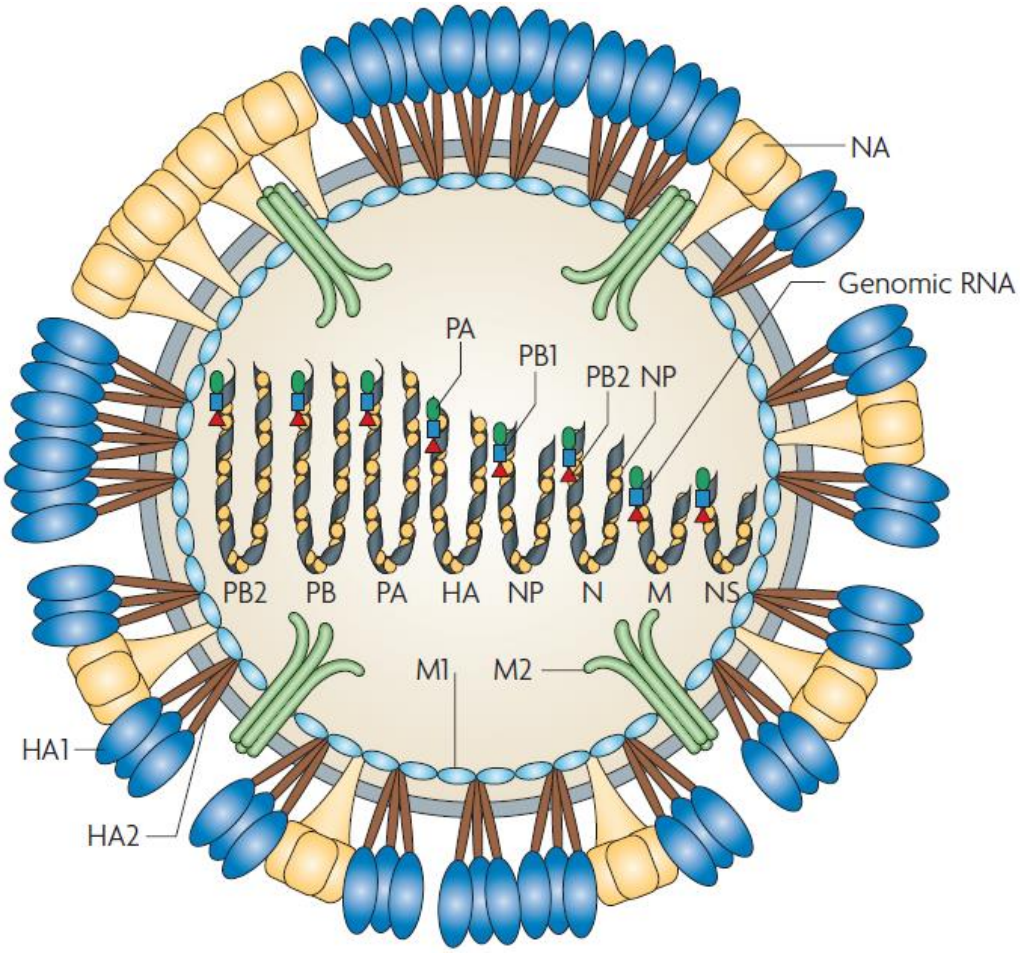

Figure 1. Overview of an influenza virion. The ribonucleoprotein core is shown here as the eight distinct segments that encode the proteins described under the segments. It is interesting to note that both M1 and M2 proteins are derived from RNA-segment 7, which means that non-silent mutations to this segment affects two structural proteins of the virus, partly explaining its conserved status. A lipid membrane (shown as a grey circle) derived from the host organism surrounds the M1-protein capsid. HA, NA and M2 are all transmembrane proteins. Adapted from [2].

After binding, virions enter their host cells in endosomes primarily via clathrin-mediated endocytosis [9]. The acidic environment in endosomes triggers a dramatic conformation change in HA that brings three fusion peptides of the trimeric protein to and through the endosomal membrane (Figure 2), effectively fusing it with the viral membrane [6]. Simultaneously, protons stream into the virion through the M2 proton channels, lowering the pH inside [11]. The change in pH weakens the interactions

between M1 and RNP, letting the viral genome escape the virion and endosome into the host cell's cytosol [3].

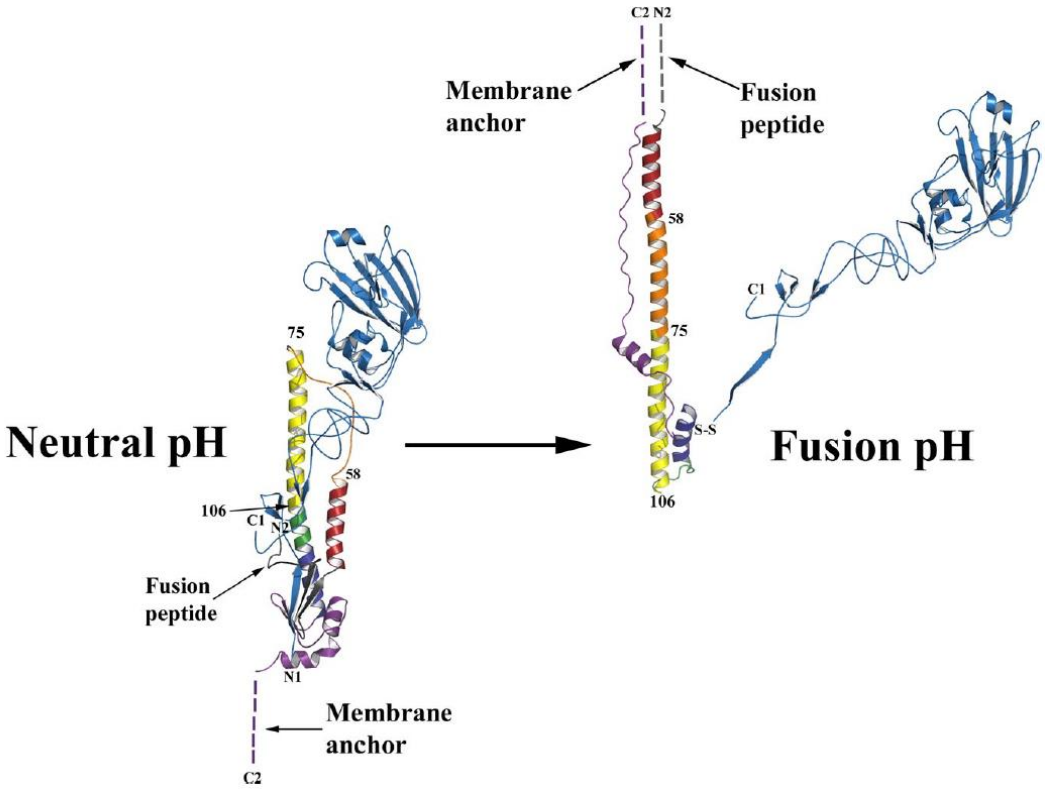

Figure 2. A conformation change in HA drives membrane fusion in low pH environments. When an influenza virus enters its host cell inside an endosome, the low pH of the organelle drives the dramatic elongation of the HA protein illustrated here. The fusion peptides of the trimeric protein penetrate the endosomal membrane and fuse it to the viral membrane. Numbers of selected amino acids, along with the termini of the two peptide chains of an HA subunit are indicated in the figure. Adapted from [18].

RNP is imported from the cytosol into the nucleus for viral RNA synthesis. Host proteins from the α-importin family recognize the targeting signals in the viral NP protein and bring RNP through a nuclear pore into the nucleus [3]. Here, viral RNA is transcribed extensively into full-length complementary copies, which are then used to create new copies of viral genomes. They are later packed into RNPs, exported from the nucleus with the help of M1 and NS2 [9] (also called nuclear export protein, or NEP) and packaged into progeny virions [7]. The viral RNA is also transcribed into mRNAs, which are 5' capped and polyadenylated by cellular machineries [3]. The viral M1 and M2 proteins derive from the same RNA segment, so the virus must also highjack the host's splicing machinery to create different mRNAs for both proteins. The synthesis of the so-called non-structural (NS) proteins from RNA segment 8 also utilizes splicing.

The transmembrane proteins of influenza, namely HA, NA and M2, are transported to the host cell membrane through *trans*-Golgi secretion [7]. The glycoproteins HA and NA gain their post-translational modifications in the Golgi apparatus [3]. In some influenza strains, like the highly pathogenic H5 and H7 viruses, HA is sometimes processed to its active form already in the Golgi apparatus [6,11]. In these influenza strains, M2 acts to raise the pH of the normally acidic *trans*-Golgi network. This reduces premature activation of the conformation change in HA. In most strains, HA is processed to its active form on the cell surface or in complete virions and M2 is not active in the Golgi network [2,6].

HA, NA and M2 contain translocation signals in their transmembrane domains that direct HA and NA to lipid rafts in the membrane and M2 to areas surrounding the rafts [9]. Lipid rafts are specific compartments in the cell membrane that contain more cholesterol and sphingolipids than the rest of the membrane, making them more rigid. The assembly of progeny virions is done at lipid rafts, and this is where RNP and the structural virus proteins are all sent for packaging. An interesting notion about the importance of lipid rafts for influenza assembly is that a natural human antiviral called viperin fights influenza by destabilizing lipid rafts and by reducing their amount [9].

M2 has many important roles in the budding and scission of new virions from the membrane. It can modify the local curvature of the cell membrane through its amphipathic helix [9]. This is used to separate new enveloped virions from the rest of the membrane. Experiments show that without M2, formed virion buds are unable to part with the membrane (e.g. [19,20]). After the cell membrane and the virion are separated from each other, the virion may still be attached to the sialic acids on the cell surface via HA. At this point, NA serves to cleave these bonds [9], and the virus progeny can finally escape its host to infect new cells.

3.1.2 Hemagglutinin as an antigen

HA is one of the large glycoproteins of influenza that occupies most of the surface of an influenza virion, alongside with neuraminidase [1]. HA is initially produced as HA0, which is then proteolytically cleaved into HA1 and HA2 by furin-related proteases in the Golgi apparatus [6] or by serine proteases on the surface of the host cell or on complete virions [2]. HA can undergo its conformation change only after it has been activated by

this cleavage event. HA2 comprises most of the stem of the protein, while the head domain is comprised entirely of HA1.

Since HA and NA are so dominant on the surface of virions, both natural and (conventional) vaccine-derived immune responses mostly produce antibodies against the head domains of HA and neuraminidase proteins [6]. These antibodies neutralize the virus mainly by preventing its sialic acid binding step [2]. Influenza has developed many strategies to elude this most common defense against it. HA and NA are heavily N-glycosylated, which protects the active protein domains from antibody binding [2]. Also, the receptor-binding domain of HA is a lot smaller than the smallest epitopes. This allows for antibody-escaping mutations in the sequence areas surrounding the receptor binding site without hindering the receptor binding capability of the virus. Overall, the head domains of HA, as well as of NA to a lower extent, are under continuous and rapid evolution. Vaccines that elicit antibodies against these proteins need to be renewed annually, and only work in a strain-specific way [2]. The stem domain of the HA protein, on the other hand, is approximately 90% conserved among the most important H1 and H3 influenza subtypes and to some extent among others [21].

An antibody discovered from a human serum sample that targets the fusion domain found in the stem has been found to neutralize all strains of influenza A [22]. A vaccine that can elicit similar antibodies effectively could potentially work as a universal vaccine. As mentioned earlier, the stem of HA is mostly comprised of the HA2 chain, so introducing this peptide chain alone to the immune system should produce the desired immune response. Producing HA2 independently has proven difficult, however. It contains the fusion peptide that is needed for the low-pH conformational change of the protein, and thus its pre-fusion form is not stable without the HA1 chain [23]. HA in its activated fusion form is only found in endosomes, so this conformation is not an attractive target for antibody neutralization. Indeed, the known antibodies that neutralize several subtypes of influenza virus all only recognize the pre-fusion form of the protein [22], which means that keeping HA2 in this conformation is imperative for an HA-vaccine to work.

To solve this problem, Bommakanti et al. [21] designed a headless HA protein that included some stabilizing fragments of the HA1 chain in the stem domain of the protein,

attached to the most conserved regions of HA2. They also introduced point mutations that stabilized the pre-fusion conformation. According to the authors, this is the first "headless" HA protein that can be produced stably in this conformation. The design of the 258-amino-acid HA stem protein was developed further by minimizing it down to 139 amino acids by exclusively selecting the fragments that were calculated to be closest to the epitopes of known broadly neutralizing epitopes against influenza [24]. This HA stem protein were based on the HA from an H1 influenza strain but the same group later developed another ministem protein based on an H5 strain [12]. The group called the H1N1-derived HA ministem protein "H1F", and this is the abbreviation used in this text from here on. The "F" in the name comes from a Foldon domain that was attached to the C-terminus of the protein. It is a small protein domain extracted from bacteriophage T4 that promotes efficient trimerization [24]. HA is trimeric in its native form, so trimerization of the recombinant vaccine may also be important for its function.

3.1.3 Matrix-2 protein as an antigen

M2 is a small 97-amino-acid transmembrane protein of the influenza virus. Four M2 subunits act together to form a tetrameric pH-dependent proton channel [25]. The protein is essential for the virus life cycle, both for inserting the genome into the host's cytosol and for the formation of progeny virions. There are two antivirals called amantadine and rimantadine that inhibit the proton-channeling activity of M2 [6]. They both affect non-conserved amino acids around the transmembrane domain, though, and escape mutants appeared quickly after the drugs were launched [26].

The first 24 amino acids in the N-terminal of M2 make up the ectodomain [11], twenty residues in the middle form the transmembrane domain and the C-terminal amino acids (44–97) are intravirional (http://www.uniprot.org/uniprot/P06821; 2.8.2017). The first nine amino acids of M2e share their open reading frame (ORF) with the M1 capsid protein, and are completely conserved (except for a single amino acid in some bat strains) [6]. The rest of the sequence shows some mutations between different influenza strains but is still conserved to a very high degree (>94%) [11]. The amino acid sequence (Figure 3) chosen for the M2e-based influenza antigens in this thesis work is the human consensus sequence [6,27].

```
Consensus of human seasonal       : MSLLTEVETPIRNEWGCRCNDSSD
A/California/07/2009              : ----------T-S--E---S----
A/Vietnam/1203/2004 (avian H5N1)  : ----------T----E---S----
```

Figure 3. Sequence alignment of M2 ectodomains off a consensus sequence and two different influenza strains. The consensus sequence selected for the vaccine candidates in this study is the same for the human H2N2, H3N2 strains and the circulating H1N1 strain before 2009. However, the H1N1 pandemic of 2009 (second row) has replaced the previous H1N1 strain and contains the shown avian-like mutations in M2e [6].

By itself, M2e is too small a peptide to cause an effective immune response [6], so it must be used with an adjuvant or some larger carrier molecule in vaccine applications. In influenza virions, there are only a few M2 proteins, but infected cells have an abundance of M2 on their surface [1,9] This means that M2-specific antibodies are unlikely to prevent infections altogether, but they are thought to protect against disease morbidity and mortality by eliminating infected cells and the virions within through antibody-dependent cellular cytotoxicity, phagocytosis and complement-dependent cytotoxicity [6].

M2e has been considered a promising candidate as a universal antigen for years already, and a few M2e-based vaccine candidates have even progressed to clinical trials. For example, an M2e-flagellin vaccine by VaxInnate Corp. (New Jersey, USA) was safe and immunogenic in phase I trials and is currently on track to phase II trials [6]. A vaccine that contains M2e displayed on the surface of hepatitis B VLPs (Sanofi Pasteur Biologics Co, Massachusetts, USA) has also shown promise in phase I trials and in lethal challenge studies done in ferrets [11].

3.2 Avidins

Avidins are a group of proteins that are best known for their ability to bind the vitamin D-biotin with great affinity ($K_D \approx 10^{-15}$ M) [28,29]. Biotin is a very wide-spread vitamin that is found in virtually all organisms. Its biological roles include working as a cofactor for carboxylase enzymes [30] and being attached to proteins in regulatory purposes [31]. In *E. coli*, a biotin ligase called BirA catalyzes specific biotinylation of a subunit of the Acetyl-CoA carboxylase enzyme [30]. The natural biotinylation target of BirA is a polypeptide of 75 amino acids, but as a result of engineering, a mere 15-amino-acid-long, stronger target substrate was found. This peptide, named AviTag, can easily be fused to recombinant proteins to achieve up to 100% biotinylation in the presence of BirA [32].

In addition to biotin-binding, other notable properties of avidin proteins are their extensive stability over wide ranges of temperatures and pH values and even resistance against proteolytic enzymes [31]. Avidin was originally found in chicken egg white, but analogous biotin-binding proteins have later been found in numerous other species as well [33]. The prototypic chicken avidin is a homotetrameric protein that contains a single biotin-binding pocket in each of its four subunits [34]. The subunits consist of eight antiparallel β-strands arranged into a classical β-barrel fold [31].

The robustness of avidin proteins and their practically irreversible biotin-binding capabilities make avidin an attractive candidate in many applications. Clinical uses of avidin have already been studied in e.g. a vaccine platform application [14] and as a carrier of pharmaceutics through the blood brain barrier [35]. The same properties have made avidin-biotin technology an active field of research for decades, and currently a lot of engineered avidins and tools based on avidin-biotin technology are readily available [28,31]. A key tool concerning this thesis work is an efficient protein purification method based on this technology. The avidin-biotin bond is practically irreversible, but avidin binds a biotin derivative, 2-iminobiotin, in a pH-dependent way [31]. This molecule is commercially available linked to a chromatography resin by e.g. Affiland S.A. (Ans Liege, Belgium). Avidin can be bound to this resin in basic conditions and accurately eluted by lowering the pH in an efficient affinity chromatography method.

In the current project, we decided to use an engineered form of chicken avidin (referred to simply as "**avidin**" from here on), whose stability and biotin-binding properties have been enhanced and whose surface charge has been neutralized by point mutations in previous studies [34,36,37]. Because we had concerns about the incompatibility of tetrameric avidin and our large, trimeric HA antigens, we decided to add two more kinds of biotin-binding proteins to our fusion protein repertoire. For this, we chose the dimeric **rhizavidin** and a recombinant, monomeric form of it that its inventors call monodin. Rhizavidin was found from a nitrogen-binding bacterium called *Rhizobium etli* [38]. According to its finders, rhizavidin is the first known naturally dimeric avidin-like protein. It binds biotin almost as strongly and specifically as avidin but is not as thermostable. In later studies, rhizavidin was subjected to some point mutations that

transformed it into a monomeric protein, dubbed "**monodin**" by its inventors [39]. Engineering a monomeric form of avidin has been achieved before [40], but with significant reductions in biotin-binding affinity. Monodin still binds conjugated biotins with almost as strong an affinity as multimeric avidins do. Its ability to bind free biotin is somewhat weaker, however.

3.3 SpyCatcher/SpyTag

In recent years, research on isopeptide-forming proteins has yielded several engineered protein-peptide pairs that can be used in bioconjugation applications [41]. Isopeptide bonds are peptide bonds (a.k.a. amide bonds) that connect two protein chains to each other, instead of extending a single peptide chain. The pilin subunit Spy0128 from the bacterium *Streptococcus pyogenes* is the first of many proteins discovered that are capable of forming isopeptide bonds within themselves [42]. Intramolecular isopeptide bonds provide these proteins with stability in changing pH and thermal conditions and protection against proteolytic enzymes [41]. In eukaryotes, similar stability-increasing properties are gained by intramolecular disulfide bonds, but many bacteria lack the enzymes and the oxidizing environment required for their formation.

One of the most promising of isopeptide-forming protein systems is the SpyCatcher/SpyTag system. The system, whose name draws inspiration from the prototypic isopeptide-forming protein Spy0128, is derived from the immunoglobulin-like collagen adhesin domain (CnaB2) of the fibronectin binding protein (FbaB) of *Streptococcus pyogenes* [43]. Zakeri et al. (2012) split the protein domain into a 13-amino-acid peptide called SpyTag and a 138-amino-acid-long (15 kDa) protein called SpyCatcher. In the original protein, SpyTag forms most of a β-strand in a β-sheet and contains a reactive aspartic acid residue that forms an isopeptide bond with a lysine residue in SpyCatcher [43]. It was discovered that after rational modification of the protein and the peptide, SpyCatcher and SpyTag could regenerate this β-sheet structure and covalently bind through the isopeptide bond in mere minutes and under various circumstances. Further optimization of the SpyCatcher protein proved that the reconstitution of SpyCatcher and SpyTag works in a near identical efficiency even though the protein is truncated by 9 amino acids from its C-terminal and by 23 amino

acids from its N-terminal [44]. This optimal SpyCatcher protein is 109 amino acids long (~15 kDa).

The SpyCatcher/SpyTag system offers an efficient way of linking different molecules together. SpyTag can be genetically fused to either terminus or even as an internal part of a target protein [43]. SpyCatcher can also be fused to either termini of a fusion partner because of its efficient and independent folding mechanism [13,43]. Because SpyCatcher and SpyTag can be flexibly fused to fusion partners, produced separately and then just mixed together to permanently bind the components to each other, they offer a robust system to fuse VLPs to desired antigens in the production of modular VLP vaccines.

3.4 Vaccines based on virus-like particles

The protein shells that surround viral genomes are composed of one or more different viral structural proteins, depending on virus species. When these proteins are expressed in a cell, they can self-assemble into a symmetrical virus capsid that usually consists of over a hundred subunits [45]. Structural proteins of many virus species can form capsid structures devoid of DNA or RNA [1], called virus-like particles (VLPs). Naturally formed VLPs were described for the first time already in 1968 [46]. Since then, the potential of these biological nanoparticles has been widely recognized.

VLPs are superb compared to "traditional" nanoparticles in many aspects. For example, they are biocompatible, stable, capable of self-assembly and the structures of many VLPs have been defined on the level of atoms. VLP research aims to numerous different applications. Many of these use VLPs as carriers of other molecules, which can either be packed inside them like viral genomes, or attached on the surface of VLPs. Applications of VLP technology include using them as biomaterials, carriers of pharmaceuticals and imaging. Still, the most popular use of VLP technology lies in vaccination.[47]

VLP-based vaccines are safe and efficient compared to traditional vaccination approaches. VLPs do not contain viral genomes, so they are unable of causing infection, whereas reversion of live attenuated vaccines to virulent forms has been one of the main concerns in the regulation of vaccines in the past. When fighting quickly evolving pathogens like influenza, it is useful to target conserved areas of the pathogen by using them as vaccines. Subunit vaccines that are comprised only of conserved epitopes tend

to be small, however. Even the subunit vaccines based on the largest proteins often fail to cause an effective immune response [45]. This can be circumvented by using additives that boost or redirect the immune response (adjuvants) in the vaccine or by using multiple injections. A more elegant approach is to present these conserved subunits on the surface of VLPs or as VLPs themselves (in the case of viral structural proteins). Like natural viruses, VLPs are robust and of the right size (20–200 nm) for being taken into antigen-representing cells and for draining into lymph nodes [13]. VLPs can be decorated in a very rigid and uniform way, and they can then crosslink B-cell receptors, an important phenomenon in creating a powerful B-cell response [48]. VLP-linked antigens can be presented in both type I and II major histocompatibility complexes (MHCs), and so they are able to activate both cytotoxic and helper T cell responses [48].

Many different VLPs have been produced for vaccine purposes. Hepatitis B VLPs, which were the first ones discovered [46], have been a particularly active field of research. They have been decorated with Zika virus and Ebola antigens, among others [49]. There are even commercially available vaccines that are made of hepatitis B [13] or human papilloma virus[50] VLPs. VLPs have been manufactured in bacterial, mammalian, avian and in plant-based and yeast-based expression systems, but insect cell systems are used most in vaccine production [47]. Insect cells can be easily infected with insect-specific baculoviruses that are safe for vertebrates, and they offer relatively inexpensive and scalable protein expression with eukaryotic post-translational modifications [13].

Noroviruses are a genetically diverse group of pathogens that are one of the main causes of gastroenteritis [51]. They have genomes of single-stranded, positive sense RNA with three ORFs. The virus capsid is almost completely comprised of the VP1 protein, which is encoded by ORF2 [52]. Recombinant expression of VP1 in cells yields empty VLPs similar to native noroviruses in size and morphology. The norovirus-like particles (noro-VLPs) are about 40 nm in diameter, and are comprised of 90 dimers of VP1 [53]. High yields of noro-VLP can be obtained from insect cell, yeast and plant-based expression systems [53]. Earlier strategies of noro-VLP purification have been based on ultracentrifugation techniques like sucrose and CsCl gradients, but these are difficult to scale up and time-intensive [52]. Koho et al. [52] described an efficient method of expressing noro-VLPs in insect cells and purifying them with ion exchange

chromatography, and later a method for making HisTagged noro-VLPs [53], which enabled both the use of affinity chromatography or VLP purification and decoration of the particles via Tris-NTA. Noro-VLPs have long been important for human norovirus studies, since the viruses could not be cultivated *in vitro* until as late as 2015 [54]. The research on norovirus structure (e.g. [55]), morphology [56] and vaccine candidates [57,58] was primarily based on noro-VLPs before this. A noro-VLP-based vaccine against norovirus itself has proceeded to phase II trials, but no reports of decorating whole noro-VLPs with foreign antigens were found at the time of writing this thesis [59].

4 Aims of the study

The proposed research aimed to produce and characterize noro-VLPs and influenza antigens, which could be bioconjugated together by plug-and-go approaches. Separate production of the antigens and VLPs would thus allow for rapid generation of new vaccines.

The specific aims of the study are:

1. To develop, produce and purify AviTagged noro-VLPs and influenza-avidin fusion protein constructs
2. To develop, produce and purify SpyTagged noro-VLPs and influenza-SpyCatcher fusion protein constructs
3. To decorate the produced noro-VLPs with the antigens.

HisTagged noro-VLP has been previously constructed and used to immobilize fluorescent dye molecules and streptavidin-biotin Tris-NTA conjugates on the surface of the modified VLPs [53]. During this study, we constructed new noro-VLPs, in which SpyTag or AviTag substituted the HisTag. Additionally, different influenza antigens fused either to SpyCatcher or recombinant avidin were produced. The former system allows covalent linking of noro-VLP carrier and antigen, and the latter the utilization of the high-affinity avidin–biotin bridge for VLP–antigen conjugation. Figure 4 shows the workflow of modular vaccine development with the SpyCatcher vaccine type as an example.

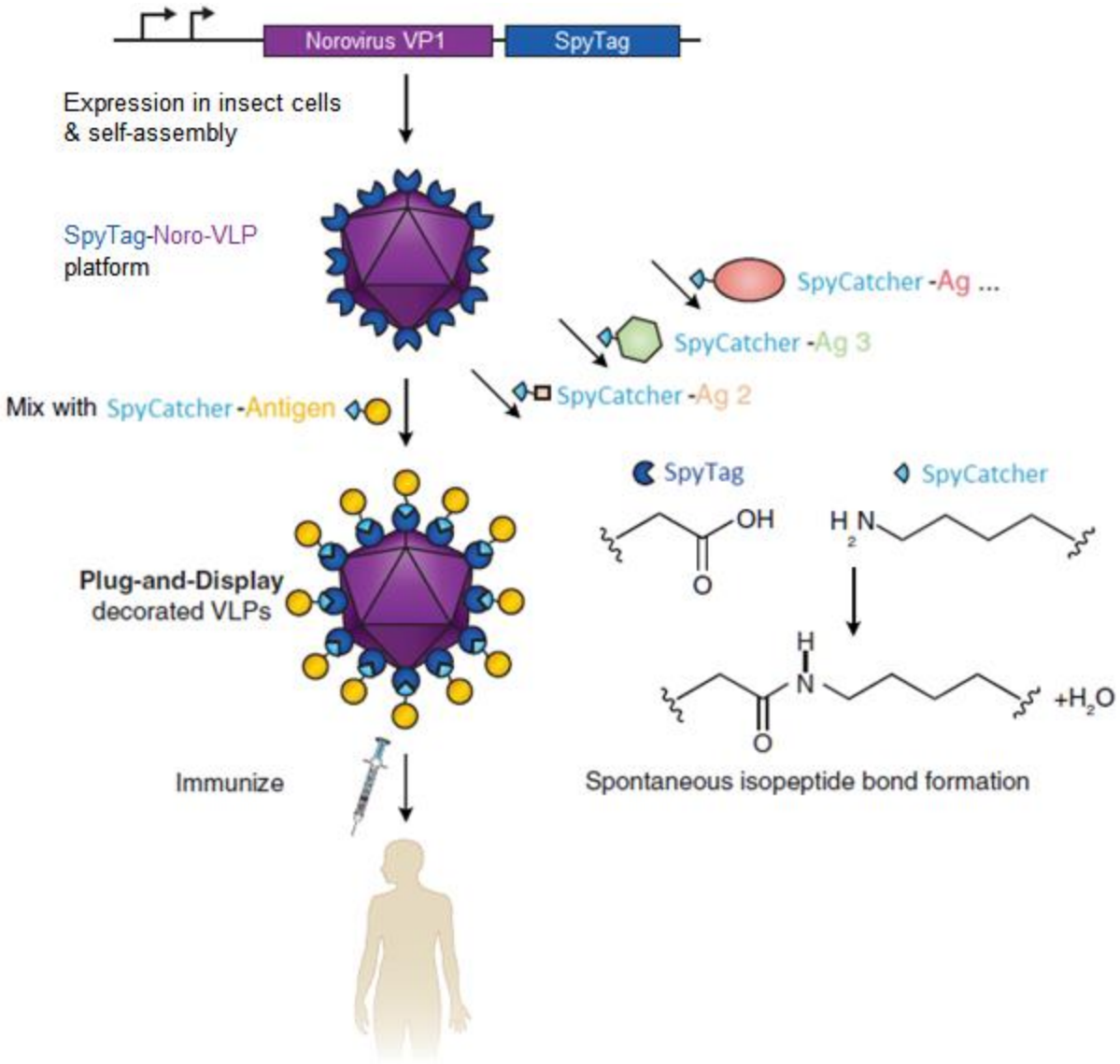

Figure 4. Norovirus-like particle vaccine design. When SpyTagged norovirus VP1 protein is expressed in insect cells, the proteins readily assemble to form norovirus VLPs with SpyTag peptides protruding from their surface. When these noro-VLPs are mixed with a SpyCatcher-antigen fusion protein, a biologically irreversible covalent bond forms in between. The antigen-decorated VLPs can then be used in vaccines. Modified from [13].

5 Materials and Methods

5.1 Antigen production

5.1.1 Antigen expression

Synthesis and amplification of antigen plasmids

The DNA sequences encoding the eight designed antigen constructs (described in Chapter 6.1.1, p. 32) were codon-optimized for *E. coli* and manufactured as synthetic genes by a commercial service provider (GenScript, Piscataway, USA). The same company subcloned the inserts into the pET-11b(+) plasmid, between the XbaI and BlpI restriction sites, and verified the success of plasmid preparation by sequencing and gel electrophoresis. The plasmids were delivered in lyophilized form and dissolved into TE (Tris-EDTA) buffer[a] upon reception.

After dissolving the plasmids, TOP10 *E. coli* were transformed with them to generate larger stockpiles of plasmid DNA. The heat shock method (30 s, +42 °C) was used to introduce the plasmids into competent bacteria. Successfully transformed bacteria were selected based on their growth on an ampicillin-glucose-LB (Amp-Gluc-LB) plate and isolated colonies were inoculated in liquid Amp-Gluc-LB medium. The liquid bacterial cultures were grown in +37 °C and with constant shaking (225 revolutions/min), if not stated otherwise. These seed cultures were grown overnight and then diluted into a large amount of fresh medium with identical composition.

After sufficient bacterial growth, we extracted the plasmid DNA with NucleoBond Xtra Midi Plus kit (Clontech, Mountain View, CA, USA). The first Midiprep attempts were made according to the kit's instructions for high-copy number plasmids, but they resulted in poor yields. After this, the seed cultures were always cleared of secreted βlactamase by centrifugation (4000 g, 10 min) and resuspension into clean medium before starting the larger cultures. This prevents plasmid loss when using ampicillin selection [60]. With this culture method improvement and switch to low-copy number

[a] 10 mM Tris, 1 mM EDTA, pH 8

plasmid protocol, plasmid yields were significantly improved and good stockpiles could be established for storage in TE buffer and -20 °C.

Optimization of the antigen expression systems

For studying protein expression levels in different *E. coli* strains and temperatures, all the plasmids were transformed into *E. coli* strains C41, C43 and BL21 Star with the heat shock method (30 s, +42 °C). Isolated colonies were extracted after growing on Amp-Gluc-LB plates and they were inoculated into 5 mL of Amp-Gluc-LB. After growing the seed cultures overnight, they were pelleted (4000 g, 10 min) and resuspended into fresh medium. Each solution was diluted 1:10 into 30 mL of Amp-Gluc-LB. The production cultures were grown until the optical density (OD) of the solution was approximately 0.5 when measured at a wave length of 600 nm. Protein expression was induced by adding isopropyl β-D-1-thiogalactopyranoside (IPTG) to a final concentration of 1 mM. Each production culture was then divided to three cultures of 10 mL, which were grown overnight in +18, +25 or +37 °C.

After ~20 hours of cultivation, 1 mL samples of the cultures were centrifuged in a tabletop centrifuge (10,000 g, 2 min) and the bacterial pellets were lysed with the EasyLyse solution (Epicentre, Madison, USA), according to the manufacturer's instructions [61]. After lysis, the resulting solutions were centrifuged (10,000 g, 5 min) and samples (called **Pellet, P**) were collected from the insoluble fraction. In the case of avidin-antigen constructs, the soluble fractions were mixed with phosphate-buffered saline[a] (PBS)-washed D-biotin sepharose 6 fast flow resin (Affiland, Ans Liege, Belgium). With SpyCatcher-antigens, the soluble fractions were mixed with PBS-washed Protino Ni-NTA Agarose resin (Macherey-Nagel, Düren, Germany). The solutions were agitated for 2 hours at room temperature to let the proteins bind the resin. The resin and the proteins bound to it (sample called **Resin**) were separated from the rest of the solution (**Flow-through, FT**) by centrifugation (20,000 g, 5 min). **Resin** was washed at this point with PBS and a further round of centrifugation. Finally, it was resuspended in PBS to get a similar volume with the other samples. The samples were analyzed with sodium dodecyl sulfate polyacrylamide gel electrophoresis (SDS-PAGE) and Stain-free protein

[a] 137 mM NaCl, 2.7 mM KCl, 10 mM Na_2HPO_4, 1.8 mM KH_2PO_4, Ph 7.4

detection by UV-induced fluorescence (details in Chapter 5.5.1, p. 26) for comparison of protein expression levels.

Avidin fusion proteins were expressed also in *E. coli* BL21-AI. After transformation, the fresh transformants were cultured in Amp-Gluc-LB medium, supplemented with tetracycline to specifically select for this strain of *E. coli*. Expression of our target proteins was induced at OD of 0.4 by adding IPTG and L-arabinose to final concentrations of 1 mM and 0.2%, respectively. Expression continued for ~20 hours at +28 °C. The same protocol was applied for rhizavidin and monodin constructs, with the exceptions of inducing at OD≈0.3 and expression at +26 °C, according to the protocol described in [38].

After analyzing the protein expression levels, optimal strains and production temperatures for the SpyCatcher-antigen proteins were established. Glycerol stocks were prepared from the best-performing colonies and stored at -80 °C. In the following protein expression studies, we always started from freshly plated (less than a week old) colonies or from the glycerol stocks.

To study optimal induction time of protein expression for SpyCatcher-M2e and SpyCatcher-H1F, 100 mL production cultures of the best transformants were prepared as described above. Subcultures of 10 mL were extracted from the larger culture vessels and induced (with 1 mM IPTG) for overnight protein expression in each protein's optimal temperature when OD reached values of 0.2, 0.4, 0.6, 0.8 and 1.0. The best induction times were established by lysing the bacterial pellets as described above, and analyzing the samples with SDS-PAGE.

Additional production cultures of 50 mL were made to test the effect of different IPTG concentrations. When the optimal OD of each protein was reached, the bacteria were again divided into subcultures of 10 mL, and expression was induced with a final concentration of 0.01, 0.1, 1 or 10 mM IPTG. The protein expression levels were analyzed with SDS-PAGE.

5.1.2 Antigen purification

For large-scale expression of SpyCatcher-M2e and SpyCatcher-H1F, we expressed the proteins in cultures of 500 mL in optimal conditions. The bacteria were pelleted by

centrifugation (12,000 g, 15 min) and the pellets were resuspended in binding buffer[a]. The resuspended pellets were lysed with the Emulsiflex-C3 (Avestin, Ottawa, Canada) homogenizer using two rounds through the valve at 60–80 bar. The lysates were fractionated with centrifugation (15,000 g, 20 min) and a **Pellet** sample for SDS-PAGE was collected from the insoluble fraction. The soluble fraction was loaded on a pre-packed HisTrap FF crude column with the ÄKTApurifier 100 chromatography system (column and system by GE Healthcare, Chicago, USA) (details in Chapter 5.5.2, p. 27). A **Flow-through** sample was collected during sample loading. After sample loading, the resin was washed with binding buffer and a **Wash** sample was collected. The proteins were eluted from the column using a linear imidazole gradient in an otherwise unchanged buffer (20 → 500 mM imidazole) and divided into 3 mL fractions. We used SDS-PAGE to analyze the elution fractions from around absorbance peaks together with the **Pellet, Flow-through** and **Wash** samples.

The best fractions were pooled and dialyzed against PBS. The protein yields were then estimated by measuring the absorbance of the purified and dialyzed protein solutions at 280 nm with a NanoDrop 2000/One spectrophotometer (Thermo Fisher Scientific, Wilmington, USA). With the absorbance (proportioned to a light path (L) of 1 cm by NanoDrop software), one only needs to know the extinction coefficient (ε) and the molecular weight of the protein (MW) to estimate its concentration in a pure solution with the Beer-Lambert equation (Equation 1).

$$A = \varepsilon c L \underset{L=1}{\Longleftrightarrow} c = \frac{A}{\varepsilon} \quad \Big| \, for \frac{g}{L}, multiply\ with\ MW$$

Equation 1. The Beer-Lambert equation. The *c* here means concentration in mol/L. When transforming to g/L, it is enough to multiply this with the molecular weight (MW) of the protein. *ε is the extinction coefficient, L is the length of the light path in centimeters and A is the measured absorbance.*

[a] 50 mM NaH_2PO_3, 500 mM NaCl, 20 mM imidazole, pH=7.5

5.2 Norovirus-like particle production

5.2.1 Norovirus-like particle expression

Synthesis and amplification of plasmids

Pre-designed gene constructs for SpyTagged and AviTagged noro-VP1 and BirA were codon-optimized for insect cell expression and manufactured as synthetic genes by a commercial service provider (Geneart, Invitrogen, USA). The VP1 sequence used was from norovirus strain Hu/GII.4/Sydney/NSW0514/2012/AU (GenBank ID: AFV08795). GII.4 has been the dominant genotype of norovirus since the 1990's, and still causes most of norovirus-associated diseases yearly [62].

The peptide tags reside in the C-termini of VP1, and they are separated from VP1 by a SpeI restriction site and a linker peptide of two glycines. The inserts were subcloned into pFastBac Dual plasmids by Geneart. SpyTagged and AviTagged noro-VP1 (Spy-noro-VP1 and Avi-noro-VP1) were cloned under the polyhedrin promoter, between BamHI and HindIII restriction sites. BirA was cloned into the same pFastBac Dual plasmid as Avi-noro-VP1, under the p10 promoter and between the XhoI and NheI restriction sites. Co-expression of BirA and its target, AviTag, fused to noro-VP1 should ensure specific and efficient biotinylation at the AviTag. The success of plasmid preparation was verified by sequencing and gel electrophoresis at Geneart. The plasmids were delivered in lyophilized form and dissolved into TE buffer upon reception. The plasmids were amplified in TOP10 *E. coli* and extracted with the high-copy plasmid protocol of NucleoBond Xtra Midi Plus kit (Clontech, Mountain View, CA, USA), as described above for antigen plasmids. Plasmid stockpiles were stored at -20 °C.

Creation of baculovirus stocks

The Spy-noro-VP1, Avi-noro-VP1 and BirA genes in the two pFastBac plasmids were translocated to bacmids in DH10Bac *E. coli* according to the Bac-to-Bac protocol [63]. The protocol is described in more detail in Chapter 5.5.4 (p. 28). Verification of transposition was obtained by PCR amplification and electrophoresis experiments. Insect cells were transfected with the PCR-verified bacmids containing the genes for either Spy-noro-VP1 or Avi-noro-VP1 and BirA. The transfections were done using the baculoFectin II reagent (Oxford Expression Technologies, Oxford, UK), according to the

baculoFectin II User Guide [64]. BaculoFectin II is based on DNA-binding porous nanoparticles that promote uptake of DNA by the cells and protect it from lysis (https://oetltd.com/product/baculofectin-ii/; 26.3.2018).

500–1000 ng of either Spy-noro-VP1 or Avi-noro-VP1 (+BirA) bacmid was mixed with baculoFectin II, and the mixture was added on $1{\cdot}10^6$ Sf9 cells adhered to a well of a 6-well plate. The cells were observed with an optical microscope 6 days post infection (dpi) and swollen cells (sign of baculovirus infection[64]) were detected. The supernatants (**P1 s**tocks) were collected and 200 µL of each was used to transfect $10{\cdot}10^6$ Sf9 cells in 10 mL of insect cell medium. **P2** stocks contained even more swollen cells 6 dpi, and again the supernatant was collected.

We acquired an approximately 1-year-old P2 stock of baculovirus that encodes wild-type (WT) noro-VP1 from the University of Tampere Vaccine Research Center for use as a control. The stock had been stored in -80 °C. All of it (~600 µL) was used to infect $22{\cdot}10^6$ adherent Sf9 cells (viability ~83%) in 40 mL of insect cell medium. WT-noro-VP1 **P3** stock was collected 3 dpi.

The infective titers of the AviTagged and Spy-noro-VP1 **P2** stocks and WT-noro-VP1 **P3** stock were estimated with the BacPAK Baculovirus Rapid Titer Kit (Takara Bio, Kusatsu, Japan), according to the manufacturer's instructions [65]. Briefly, early-log phase Sf9 cells adhered to the wells of a 96-well plate are infected with different dilutions of a baculovirus stock. Methylcellulose is added to make the culture medium semi-solid; this facilitates colony formation and their counting [66]. The baculovirus-infected cells are incubated at +27 °C for 43–47 hours before fixing, detecting and staining them with horseradish peroxidase (HRP)-conjugated anti-gp64 monoclonal antibodies and a blue-colored peroxidase substrate. The infected cell colonies become stained and can be counted under an optical microscope. The result is given as focus-forming units (FFU) per milliliter of the undiluted stock solution. [65]

When Spy-noro-VP1 and Avi-noro-VP1 **P2** stocks and the WT-noro-VP1 **P3** stock were each used to infect $50{\cdot}10^6$ Sf9 cells in 50 mL of insect cell medium at a multiplicity of infection (MOI) (meaning the ratio of the estimated number of virus particles to the number of cells) value of 0.1, signs of bacterial contamination were detected at

supernatant collection 6 dpi. The cultures were more turbid and smelly than usual and centrifugation at 4000 g for 15 min failed to clarify the supernatants. When a small amount of either of the P2 stock solutions or of the WT-noro-VP1 P3 stock were mixed with insect cell medium in sterile conditions, the solution became turbid after a few days of growth in +27 °C, even in the absence of insect cells. Bacteria were observed with an optical microscope.

Spy-noro-VP1 and Avi-noro-VP1 **P1** and WT-noro-VP1 **P3** stocks were sterilized by pushing them through a sterile Filtropur S syringe filter (Sarstedt, Nümbrecht, Germany) with a pore size of 0.2 µm. The pore size should retain the viruses in the solution but exclude possible bacterial or cellular contaminants. Filter-sterilization was routinely done to all virus stocks at collection from here on. The sterilized **P1** and **P3** stocks were used to infect $50{\cdot}10^6$ Sf9 cells in 50 mL of insect cell medium. The solutions showed no signs of bacterial contamination at 6 dpi and new AviTagged and Spy-noro-VP1 **P2** and WT-noro-VP1 **P4** stocks were collected. We estimated the infective titers of each of these baculovirus stocks with the BacPAK Baculovirus Rapid Titer Kit. These stocks were used for VLP expression studies and their titers are shown in Table 1 (p. 40)

Noro-VLP expression

Now that we had estimated the infective titers of the Spy-noro-VP1 and Avi-noro-VP1 **P2** stocks and the WT-noro-VP1 **P4** stock, they were each used to infect $100{\cdot}10^6$ Hi5 cells and $100{\cdot}10^6$ Sf9 cells in 50 mL of insect cell medium at different MOI values. There was enough baculoviruses to try MOI values of 0.5 and 1.0 for SpyTagged and Avi-noro-VP1 and 0.5, 1.0 and 5.0 for WT-noro-VP1. Sterile-filtered biotin solution was added with the Avi-noro-VP1 baculovirus to a final concentration of 50 µM to mitigate the cell-harming effects of the protein's biotin binding. At 5 dpi, the cultures were centrifuged (2000 g, 30 min) and samples from both the pellet and supernatant were analyzed with SDS-PAGE to study the effects of cell line and MOI value for the expression of each VLP protein. The supernatants were frozen and stored in -20 °C, so the noro-VLPs could be purified from them later.

We also sought to detect the noro-VLPs by Western blotting (WB) (details in Chapter 5.5.1, p. 26) of the SDS-PAGE gels. Multiple gels containing combinations of SpyTagged, AviTagged and wild type noro-VLP samples were blotted onto nitrocellulose membranes

with purified noro-VLPs from another strain (004/95M-14/1995/AU; GenBank ID: AF080551)) as positive controls. Monoclonal mouse anti-norovirus GII.4 antibodies (Kim Laboratories, Illinois, USA) at a 1:4000 dilution in TBS-T (0.05% Tween 20 (T) in tris-buffered saline[a] (TBS)) were used for noro-VLP detection. Finally, the membranes were imaged with the Odyssey system.

5.2.2 Purification of SpyTagged norovirus-like particles

A single 50 mL pilot expression (MOI 1.0) of Spy-noro-VLP was purified with the following protocol. First, the noro-VLP production supernatant was clarified using a Nalgene Rapid flow 0.2 µm vacuum filter (Thermo Fisher Scientific, Wilmington, USA). A small **Start** sample was collected, and the rest was added on top of 6 mL of 30% sucrose cushions and centrifuged for 14 hours in 175,000 g. The resulting supernatants were carefully removed, a **Supernatant** sample was taken, and the pellets were dissolved into 1 mL of PBS overnight in continuous stirring. After collecting a small **Pellet** sample, both dissolved pellets were further diluted by adding 1 mL of PBS. They were then centrifuged (13,000 g, 5 min, +4 °C), and the resulting supernatants were combined and diluted by adding 96 mL of binding buffer[b] to a total volume of 100 mL, from which a small **Load** sample was collected.

The soluble fraction was loaded on a pre-packed HiTrap SP FF cation exchange column (GE Healthcare, Chicago, USA) that was connected to the ÄKTApurifier 100 instrument. A **Flow-through** sample was collected. The proteins were eluted from the column using a gradually growing concentration of elution buffer[c], with steps of 10, 20 and 60% of elution buffer. ÄKTA was used to monitor the concentrations of eluting proteins (by monitoring UV absorbance at 280 nm) and for dividing them into 1 mL fractions. The elution fractions associated with absorbance peaks and the **Start, Pellet (P), Supernatant (Sup), Load and Flow-through (FT)** samples were analyzed with SDS-PAGE. The protein concentrations in the best fractions were estimated by using the NanoDrop device. The fractions with Spy-noro-VLP were pooled together and dialyzed against PBS.

[a] 50 mM Tris-Cl, 150 mM NaCl, pH 7.5
[b] 25 mM citrate, pH 5
[c] 25 mM citrate, 1 M NaCl, pH 5

Purified Spy-noro-VLP samples and control samples (unpurified Avi-noro-VLP supernatants and a baculovirus sample) were run on a gel, analyzed with SDS-PAGE and electroblotted onto nitrocellulose membrane for WB. The membrane was blocked with Odyssey blocking buffer (LI-COR Biotechnology, Lincoln, USA). Monoclonal mouse anti-gp64 antibody (Santa Cruz Biotechnology, Dallas, USA) (diluted 1:2000 in 2% bovine serum albumin (BSA) in TBS-T) was used for the detection of baculoviruses. The primary antibodies were then recognized with the IRDye 800CW-conjugated goat anti-mouse secondary antibody (LI-COR Biotechnology, Lincoln, USA) (diluted 1:5000 in TBS-T) using the Odyssey system.

5.3 SpyCatcher/SpyTag conjugation

To evaluate the ability of the produced and purified SpyCatcher-antigens and Spy-noro-VLPs to conjugate and form the decorated VLPs, the vaccine components were initially mixed together in their own elution buffers. We aimed for a 1.5-fold molar amount of SpyCatcher-antigen as compared to Spy-noro-VP1. After mixing, the reaction tubes were agitated for 2.5 h at room temperature and analyzed with dynamic light scattering (DLS) (details in Chapter 5.5.5, p. 30) and SDS-PAGE.

For the second round of conjugation studies, the purified SpyCatcher-M2e and Spy-noro-VLP preparations were first dialyzed into PBS and syringe-filtered (0.2 µm) to dispose of possibly agglomerated proteins. A constant amount of Spy-noro-VLP was then mixed with increasing volumes of SpyCatcher-M2e preparation, and the reaction tubes were rocked gently for 1 h in room temperature before analyzing with DLS and SDS-PAGE.

5.4 Avidin binding studies with AviTagged noro-VLP

To evaluate whether avidin can bind the AviTagged (thus, biotinylated) noro-VLP, supernatant samples of a pilot expression experiment of Avi-noro-VLP were mixed with increasing volumes of charge-neutralized chimeric avidin (CNCA) [67]. The reaction tubes were rocked gently for 1.5 h at room temperature before analyzing with DLS and SDS-PAGE. This time, the samples were warmed at +60 °C in the presence of SDS-PAGE

sample buffer[a] for 10 minutes, instead of boiling them. This was done to retain the tetrameric structure of the avidin used in conjugation.

In another experiment, pellet and supernatant samples of Avi-noro-VLP were run on an SDS-PAGE gel together with Spy-noro-VLP samples, CNCA and biotinylated BSA as controls. The gel was blotted onto a nitrocellulose membrane. The membrane was then blocked with BSA-TBS-T, and incubated in a solution containing 10 µg/mL CNCA in the blocking buffer. Unbound avidin was washed away and the bound avidin was detected with a polyclonal rabbit anti-avidin antibody (University of Oulu, Oulu, Finland) (diluted 1:5000 in TBS–T with 1% milk powder (Valio, Helsinki, Finland)). We used the IRDye 680RD-conjugated goat anti-rabbit antibody (LI-COR Biotechnology, Lincoln, USA) (diluted 1:5000 in TBS-T) to visualize the bound primary antibodies with the Odyssey CLx.

5.5 Main methods and their principles

5.5.1 SDS-PAGE and Western blotting

In SDS-PAGE analyses, the samples were mixed with SDS-PAGE sample buffer, boiled for 10 minutes and run through a polyacrylamide gel with an electric current to separate the proteins. In addition to self-made gels, Any kD Mini-PROTEAN TGX Stain-Free Precast Gels, Any kD Criterion TGX Stain-Free Protein Gels and gels made with the TGX Stain-Free FastCast Acrylamide Kit, 12% (Bio-Rad, Hercules, California, USA) were used. The stain-free gel contains a trihalo compound that covalently binds the tryptophan residues of proteins in the gel when activated by UV-light [68]. The compound enhances the fluorescence emitted by tryptophan when irradiated with UV-light to a level that allows detection of 20–50 ng of protein with at least one tryptophan residue. The stain-free gels were imaged with ChemiDoc XRS+ (Bio-Rad, Hercules, California, USA). Boiling in the sample buffer serves to denature the proteins, so their advancement through the gel is not affected by their shape. The negatively-charged SDS covers the linearized protein uniformly and dominates the intrinsic charge of the protein. As a result, proteins with shorter peptide chains advance further in the gel than longer ones.

[a] 0.25 M Tris-HCl, 715 mM mercaptoethanol, 10% SDS, 0.5% bromphenol blue, pH 8.8

The resulting gels were blotted onto nitrocellulose membranes with the Trans-Blot Turbo Blotting System (Bio-Rad, Hercules, USA) for standard Western blotting analysis with the Odyssey system. The PageRuler Unstained Protein Ladders (Thermo Fisher Scientific, Wilmington, USA) were visualized with Ponceau 'S color (Sigma-Aldrich, St Louis, USA) and marked in the membrane with a Western blot marker pen (LI-COR Biotechnology, Lincoln, USA). The extra binding sites in the membrane were blocked with proteins by incubation in a blocking buffer, then incubated with primary antibodies, which are later recognized with secondary antibodies conjugated with near-infrared fluorescent signaling molecules. The membranes were washed thrice with TBS-T between the antibody treatments and imaged in TBS with the Odyssey CLx (LI-COR Biotechnology, Lincoln, USA).

5.5.2 Chromatographic purification methods

The antigens and VLPs in the work were purified with chromatographic methods using the ÄKTApurifier 100 (GE Healthcare, Chicago, USA) instrument. The instrument was used for automatically equilibrating the pre-packed column to the binding buffer, loading the crude protein solution, washing the column and for eluting the bound proteins from the column. The ÄKTA instrument was also used to monitor the concentration of eluted proteins (by monitoring absorbance at 280 nm) and for dividing them into fractions of suitable sizes.

The HisTag in the N-terminus of the SpyCatcher-antigen fusion protein was utilized in purifying them with immobilized metal affinity chromatography (IMAC). In IMAC, Ni^{2+} (or other bivalent metal ions) are attached to a resin of agarose beads and the resin is packed into a column. The cluster of (most often) 6 histidines in the tag form coordination bonds with the bound metal ions [69]. The resin-bound proteins can be eluted by adding free imidazole, which competes with the histidine–ion interactions.

The recombinant noro-VLPs in this work were purified with ion exchange chromatography (IEX). The method is based on columns with negatively or positively charged resins, called cation or anion exchangers, respectively. The crude protein solution to be purified is loaded on the column in either a more acidic or basic buffer compared to the target protein's pI value. In a pH higher than a protein's pI, the protein surface is charged negatively and binds an anion exchanger, and vice versa. In this work, we used a buffer

with a pH (5.0) below the theoretical pI of Spy-noro-VLP (5.6) and a strong cation exchanger. The target protein was then eluted from the resin by raising the salt concentration. [70]

5.5.3 Insect cell culture

Insect cells were maintained in suspension cultures of 50 mL at +27 °C and constant shaking. The culture volumes were gradually increased before using the cells for protein expression. The cells were passaged three times per week to maintain them in log-growth phase. Both *Spodoptera frugiperda* (Sf9) and *Trichoplusia ni* (Hi5) cells were grown in Lonza Insect-XPRESS Protein-free Insect Cell Medium with L-glutamine. In the case of Hi5 cells, the medium was supplemented with heparin at a concentration of 10 U/mL to avoid aggregation of the cells. We did not use antibiotics in our insect cell cultures. Only cells with a viability of >90% were used for baculovirus amplification, for determining the virus titers and for protein production, unless stated otherwise. We used the Countess Automated Cell Counter (Invitrogen, CA, USA) to estimate the concentration and viability of the insect cells.

5.5.4 Bac-to-Bac protocol

The noro-VLPs in this study were produced with the baculovirus-insect-cell expression system. For generating the recombinant baculoviruses that can be used to infect insect cells, the genes encoding Spy-noro-VP1, Avi-noro-VP1 and BirA had to be translocated from the pFastBac Dual plasmids to baculovirus genomes. This was achieved with the Bac-to-Bac protocol, which is based on site-specific transposition of expression cassettes into baculovirus shuttle vectors (bacmids) in bacteria (Figure 5) [63]. Bacmid is a name commonly used for the baculovirus genome, which is formed by a single circular dsDNA, in protein engineering contexts. A DH10Bac *E. coli* bacterium carries a Helper plasmid and a bacmid in addition to its own chromosome. The bacmid and the Helper plasmid provide the bacterium with kanamycin and tetracycline resistance, respectively. A transposase, which can move the genes flanked by Tn7 transposition sites in pFastBac Dual to the bacmid in transformed bacteria, is expressed from the Helper plasmid. The genes are transposed into an area of the bacmid that disrupts the expression of lacZ, encoded there. Therefore, successful transformants form white colonies when grown in

the presence of X-gal and IPTG, while DH10Bac *E. coli* without the genes of interest form blue colonies in the same conditions. [63]

DH10Bac *E. coli* were transformed with ~1000 ng of each of the two different plasmids using heat shock (45 s, +42 °C). The transformation solutions were plated on LB-agar plates with kanamycin, tetracycline, ampicillin, X-gal and IPTG. Ampicillin resistance is provided by the pFastBac Dual and all DH10Bac *E. coli* are resistant against kanamycin and tetracycline (see above). The bacteria were grown for three days, after which white colonies were re-streaked on identical plates and grown for an additional day before inoculating them into 5 mL of liquid LB with the listed antibiotics. After growing the bacteria overnight, the bacmid DNA was extracted and dissolved into TE-buffer, according to the Bac-to-Bac User Guide [63].

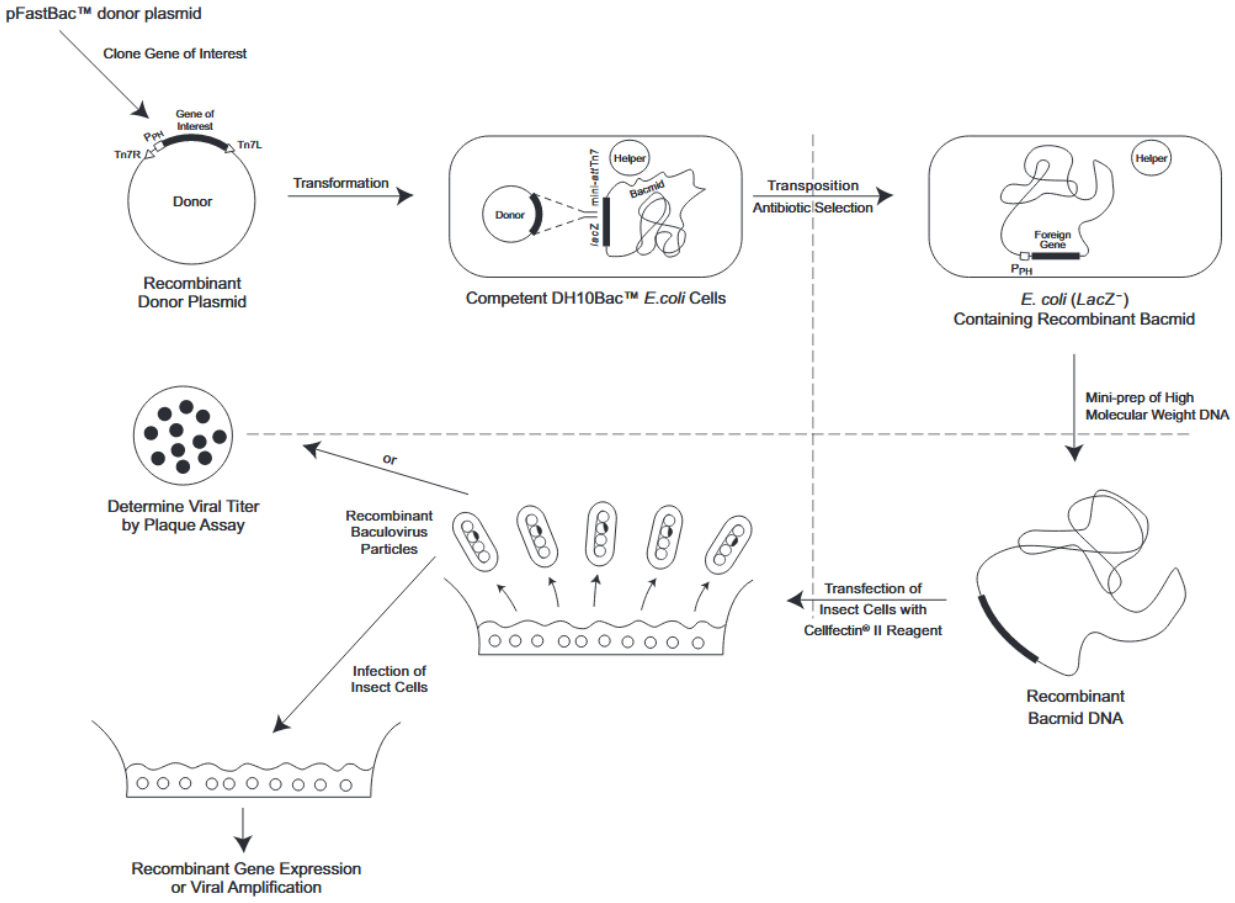

Figure 5. Overview of the Bac-to-Bac protocol. Adapted from [63].

Additional verification about the success of transposition was obtained by PCR amplification of the bacmid DNA. Two PCR reactions with different forward primers were done: in the first one, we used primers complementary to both the M13 sites that flank the mini-*att*Tn7-site (Figure 6). In this reaction, the PCR products deriving from the bacmid alone should be ~300 bp in length, while bacmids transposed with pFastBac Dual should yield products of ~2560 bp + the size of the inserts. In the second reaction, the M13 Forward primer was replaced with a primer complementary to the Tn7L site. The parental plasmid lacks this site, so no PCR product are formed. PCR products deriving from recombinant plasmids are 200 bp in size. [63] The PCR products were run on an agarose gel for size estimation.

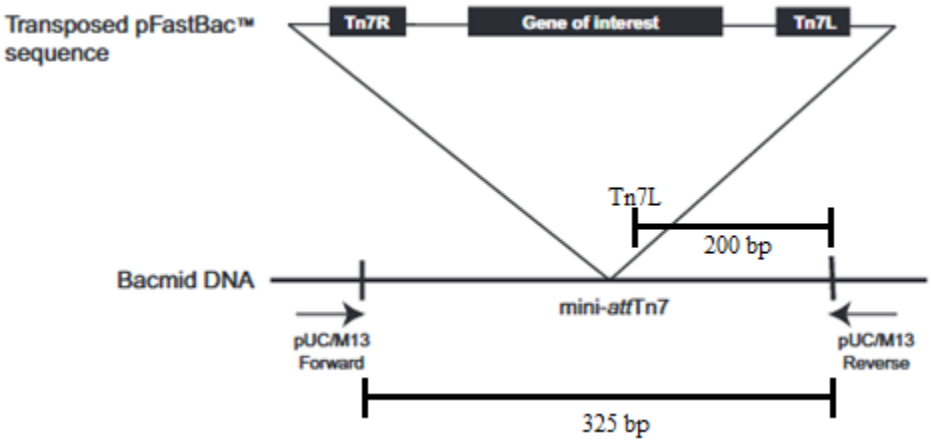

Figure 6. The principle of bacmid PCR validation. By amplifying the stretch of DNA between the M13 sites with different primers, DNA products of different length are obtained, depending on the size of the gene of interest and the success of transposition. The sizes can be estimated by agarose gel electrophoresis. Modified from [63].

5.5.5 Dynamic light scattering

The polydispersity and size of the produced and purified antigens and noro-VLPs were evaluated with DLS using Zetasizer Nano ZS (Malvern Instruments, Worcestershire, UK). The device is equipped with a HeNe gas laser with a wave length of 633 nm. The device's software gives the results in the form of the hydrodynamic diameters of the molecules in the solution with the accompanying standard errors. The results were based on cumulant analysis of three consecutive measurements, each containing 15 readings over 10-second intervals. The measurements were made at +25 °C and with a scattering angle of 173°, with predefined standard operating procedures (SOPs).

Dynamic light scattering analysis is based on the fact that small molecules move faster than large ones due to Brownian motion. When visible light hits molecules in a solution, the light scatters. A DLS device beams monochromatic light through a liquid solution and measures the amount of scattered light (Figure 7). By following the fluctuations in scattering, information about the dimensions of the molecules in the solution and its polydispersity can be calculated. [71]

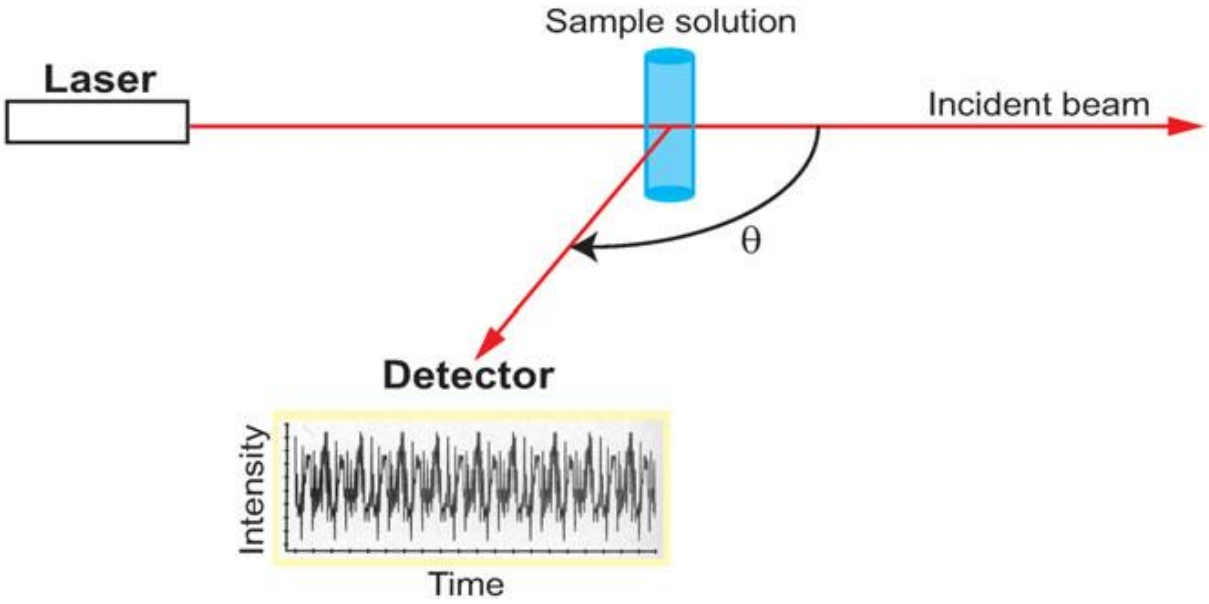

Figure 7. A schematic presentation of the setup of a DLS device. The device's laser emits monochromatic light through the sample. The light scatters from the molecules in the sample solution and scatters. The intensity of the scattered light is measured and recorded as a function of time. The detected scattering angle θ may be either fixed or changed during the measurement. Adapted from [71].

6 Results

6.1 Production of antigens

6.1.1 Antigen design

In total, we designed six different avidin-antigens and two SpyCatcher-antigens to be used in the thesis work: monodin, rhizavidin and SpyCatcher were genetically fused to M2e or H1F. We also designed an M2e fusion form of the tetrameric avidin, but for the HA ministem protein, we chose H1HA10 described in [21]. This is the same as H1F, except that it lacks the Foldon-trimerization domain. We figured that a trimerizing antigen attached to a tetramerizing molecule would be likely to cause problems in protein expression and folding. See the Appendix (p. 59) for the amino acid sequences of the designed constructs.

To produce the described influenza-antigens with their fusion partners, we first needed to design nucleotide sequences that would allow for the production of the proteins in a meaningful way. Avidins contain disulfide bonds that are essential for the function and stability of the proteins, and therefore should be expressed into the periplasm of bacteria to reach the oxidizing conditions needed in disulfide bond formation [72]. Additionally, the periplasmic space is devoid of biotin, so the produced avidins do not become saturated with biotin or harm the bacteria as much as they would in the cytoplasm.

For directing the proteins to the periplasmic secretory pathways, we included N-terminal signal peptides to our avidin constructs, according to previous experiences with the production of avidin [34,36,37], rhizavidin [38] and monodin [39]. With avidin, we used the signal peptide from the *Bordetella avium* OmpA protein (Signal peptide 3 in the amino acid sequences) [72], while the rhizavidin-M2e and monodin-M2e constructs both had a truncated *Rhizobium etli* signal peptide (Signal peptide 1) used successfully by Helppolainen et al. [38]. Before ordering the synthesis of our H1F constructs, though, we discovered a signal peptide that could allow for more efficient periplasmic production of rhizavidin [73] than the signal peptide used in the original publication by Helppolainen et al. The signal peptide that was claimed more efficient in the previous study (Signal peptide 2) is derived from a periplasmic *E. coli* protein called DsbA

(https://www.uniprot.org/uniprot/P0AEG4; 23.3.2018). It replaced the original signal peptide in our H1F-rhizavidin and H1F-monodin constructs, which are both based on rhizavidin. Production of monodin was initially done without a signal peptide using cytoplasmic inclusion-body-based expression [39].

Since the signal peptide needs to lie in the N-terminus of a protein and our research group had more experience in producing avidins with C-terminal extensions, we decided to fuse the antigens into the C-termini of avidins. With our two SpyCatcher constructs (SpyCatcher-M2e and SpyCatcher-H1F), we chose to use the same strategy according to our predictions of the structures of our fusion protein candidates. The minimized, N- and C-terminally truncated (109 amino acids) form of SpyCatcher was used. The predicted fusion structures were created with the SynLinker web application (http://synlinker.syncti.org/; 27.9.2017) and visualized with PyMOL [74] and DeepView [75]. The alternative that had the antigen fused to the C-terminus of SpyCatcher seemed to leave most space for the binding of SpyTag (Figure 8). This solution also made the different constructs more comparable with each other. HisTags were included in the N-termini of SpyCatcher constructs to allow for easy purification by IMAC. The HisTags were separated from the constructs by TEV-protease sites that allow for their removal from the proteins, if necessary.

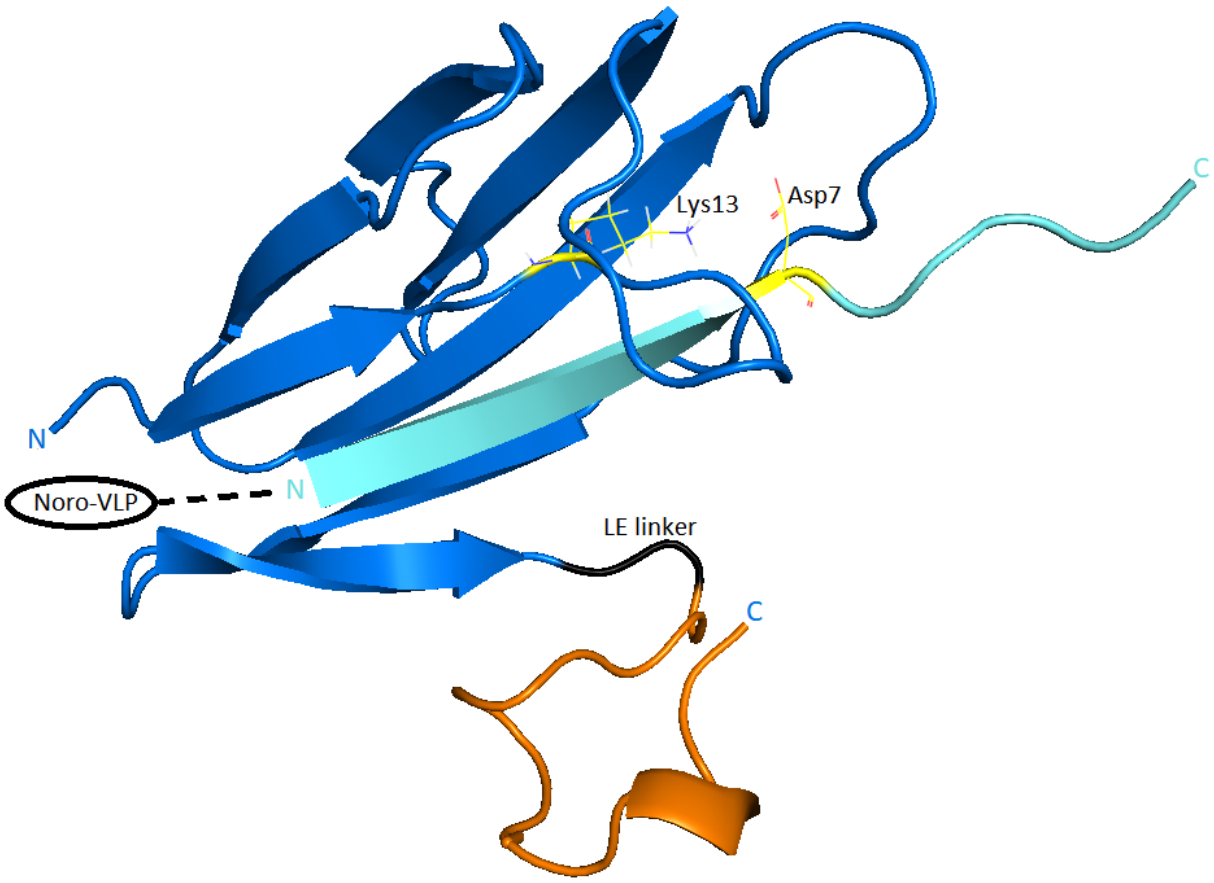

MHHHHHHDYD IPTTENLYFQ GSGDSATHIK FSKRDEDGKE LAGATMELRD SSGKTISTWI 60
SDGQVKDFYL YPGKYTFVET AAPDGYEVAT AITFTVNEQG QVTVNGLEMS LLTEVETPIR 120
NEWGCRCNDS SD** 132

Figure 8. Model structure of SpyCatcher-M2e with SpyTag in position for conjugation. SpyCatcher is colored blue, SpyTag is cyan and M2e is orange. The isopeptide bond forms between Lys13 and Asp7 (numbered from the N-termini of N-truncated SpyCatcher and SpyTag), the carbon atoms of which are shown in yellow. A leucine-glutamic acid (LE) linker, which is shown in black here connects M2e to SpyCatcher. The noro-VLP was genetically fused to the N-terminus of SpyTag, as shown in the figure. The amino acid sequence of SpyCatcher-M2e is shown below the model. The HisTag and the TEV protease site are shown in black and red, respectively, in the sequence but they are not included in the model. Other colors match the 3D model. The reactive lysine is shown in bold and underlined. The figure was created by fusing peptide chains from PDB structures 4N8C (M2e) and 4MLS (SpyCatcher+SpyTag) together with the SynLinker web application and then visualizing the structure with PyMOL.

We used the pET-11b(+) plasmid as the vector for all our antigen constructs. An XhoI restriction site was introduced between each avidin or SpyCatcher and antigen to allow for later plasmid modification. The multiple cloning site of pET-11b(+) lies under a T7 promoter regulated by a *lac* operon (http://ecoliwiki.net/colipedia/index.php/pET-11b; 22.12.2017). The lacI gene in the plasmid encodes a protein that represses the *lac* repressor in the presence of glucose and in the absence of allolactose (or its analog, IPTG). The plasmid uses a high-copy number origin of replication (pBR322), but also codes for the rop-gene, which downregulates the copy number to lower levels

(http://www.uniprot.org/uniprot/P03051; 22.12.2017). Ampicillin resistance is provided to successfully transformed bacteria by the plasmid's β-lactamase gene.

6.1.2 SpyCatcher-M2e expression

The parameters for SpyCatcher-M2e expression were optimized successfully and large amounts of protein could be produced. The effects of different production conditions were compared by analyzing the SpyCatcher-M2e proteins in SDS-PAGE with total protein staining (Figure 9). No other proteins that ran near the 15 kDa marker band could bind the Ni-NTA-resin, so SpyCatcher-M2e could be identified without a working antibody. Out of the strains and temperatures tested, BL21 Star *E. coli* appeared to produce the protein best in +25 °C. Based on the gel images, induction with 1 mM IPTG at OD≈0.6 seemed to give the largest amounts of soluble protein.

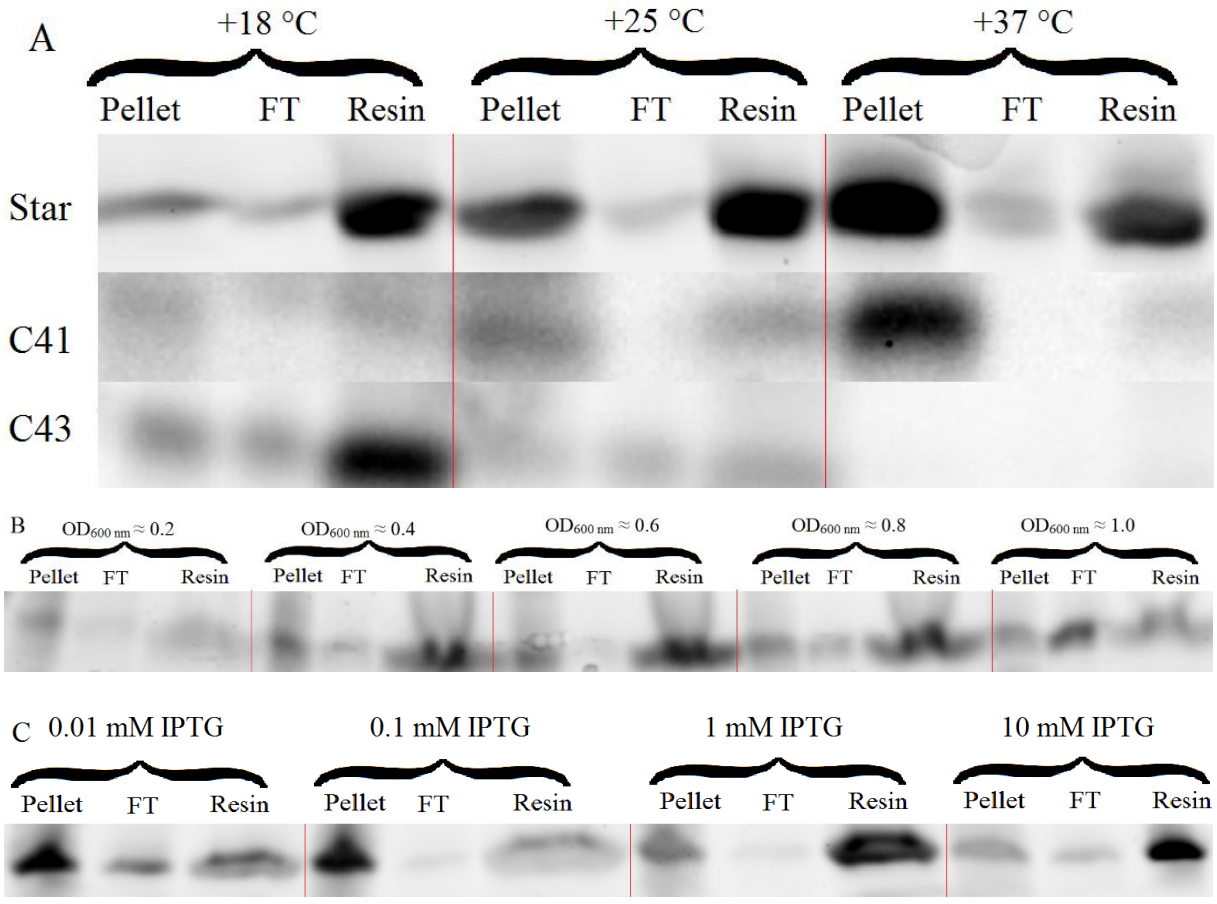

Figure 9. Optimization of SpyCatcher-M2e production conditions. A) Strain and temperature optimization for SpyCatcher-M2e. These were the only proteins in the gels that ran near the 15 kDa protein marker and bound the Ni-resin, and thus identified to be SpyCatcher-M2e. B) Induction time optimization for SpyCatcher-M2e. $OD_{600\ nm}$ means the absorption of the culture medium measured at 600 nm, i.e. the optical density of the medium. C) IPTG concentration optimization for SpyCatcher-M2e.

A 500-mL production of SpyCatcher-M2e was done in optimal conditions and purified with IMAC. SDS-PAGE analysis of the elution fractions and samples collected during the purification process shows that most impurities are removed during IMAC purification and it results in very pure SpyCatcher-M2e (Figure 10). A small amount of ~30 kDa protein can be seen in the elution fractions. Its amount seems to decrease together with SpyCatcher-M2e. No clear elution peaks were obtained when eluting SpyCatcher-M2e with a linear imidazole gradient. After pooling and dialysis of the best fractions, the total protein concentration was measured with the NanoDrop device. We obtained ~17 mg of protein, over 95% of which is SpyCatcher-M2e, according to visual analysis of the Stain-free-imaged SDS-PAGE gels. This translates to an approximate production yield of 34 mg/L. An attempt to purify SpyCatcher-M2e with sharper elution peaks by stepwise elution (steps of 60% and 100% elution buffer) ended up in a similar, constant elution rate (results not shown).

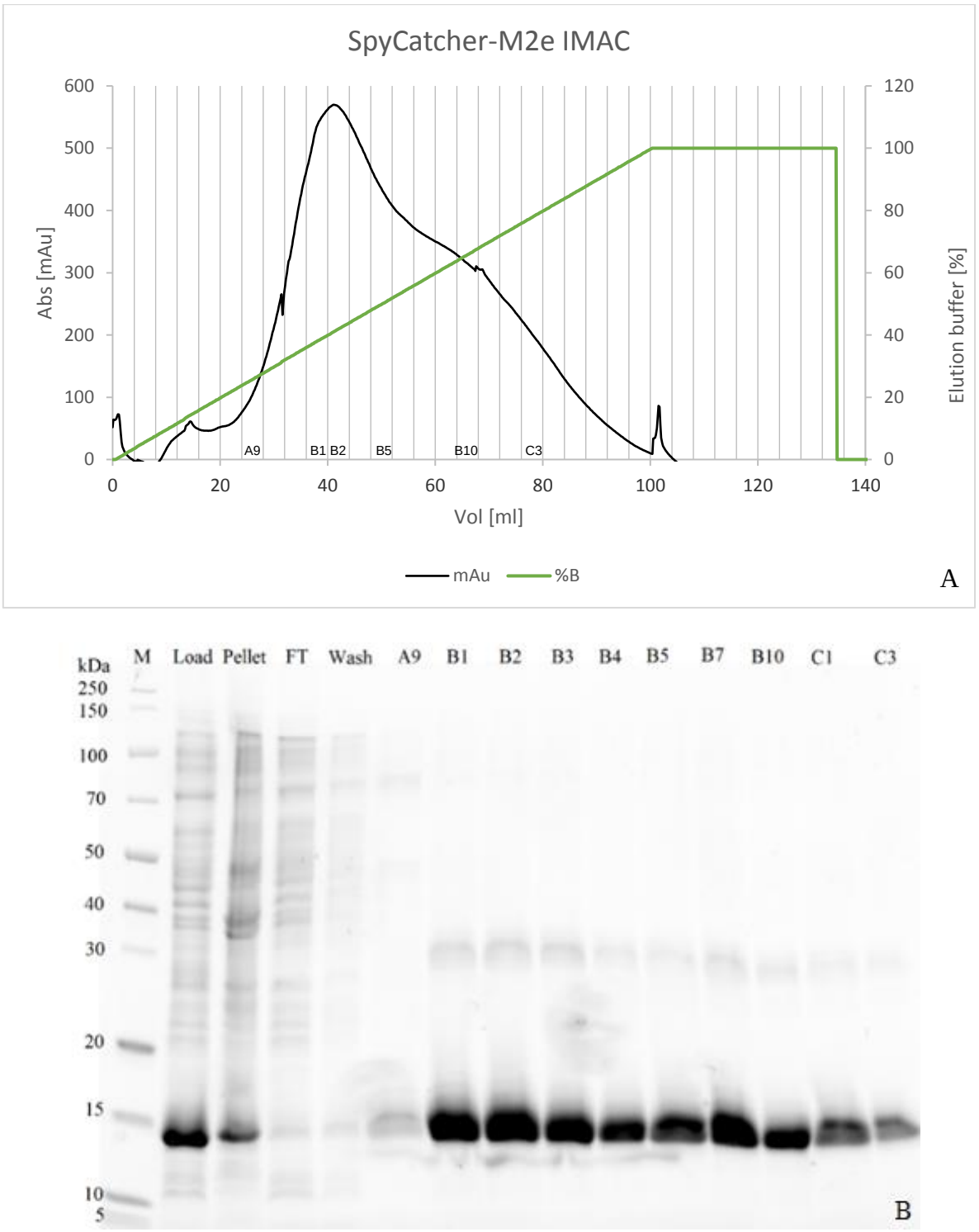

Figure 10. SpyCatcher-M2e IMAC purification. A) A chromatogram of the elution of SpyCatcher-M2e. Locations of selected elution fractions are indicated in the figure. No clear peak of SpyCatcher-M2e was obtained and it eluted evenly to a number of fractions, as seen from the solid black absorbance (Abs) line. The concentration (%) of elution buffer is shown as a solid green line. B) Stain-free image of purification samples on an SDS-PAGE gel. The M lane contains PageRuler Unstained Broad Range Protein Ladder. "Pellet" represents the insoluble fraction after lysis, "Load" is a sample of the solution loaded on the chromatography column. "FT" and "Wash" are samples of the flow-through and wash fractions from IMAC. Their collection is described in Chapter 5.1.2. The letter-number codes represent samples from elution fragments, named A, B, C, ... for the rows and 1, 2, 3, ... for the columns in the fraction collector. The collector moved in a zig-zag fashion, so every other row was fractionated from column 12 to 1.

6.1.3 SpyCatcher-H1F expression

The expression parameters for SpyCatcher- H1F were optimized in an identical way to SpyCatcher-M2e. Again, the proteins seemed to be expressed strongly from the start and production levels of the 31 kDa proteins could be followed using the SDS-PAGE gel images. After IMAC purification, over 95% pure SpyCatcher-H1F was obtained, according to visual analysis of the gel image (Figure 11). The production yield was estimated at ~27 mg/L.

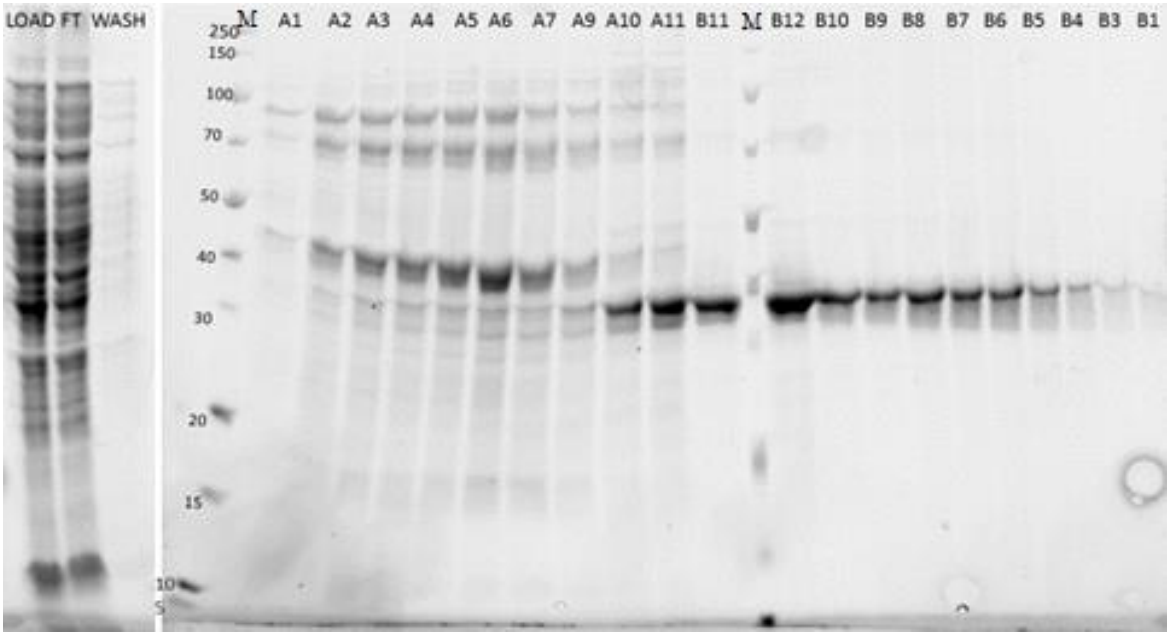

Figure 11. SpyCatcher-H1F IMAC purification. Samples from SpyCatcher-H1F purification were analyzed with SDS-PAGE and Stain-free imaging. SpyCatcher-H1F is a 31 kDa protein and the only one on the same level as the 30 kDa marker here. Lanes labeled M contain PageRuler Unstained Broad Range Protein Ladder. "Load" is a sample of the solution loaded on the chromatography column. "FT" and "Wash" are samples of the flow-through and wash fractions from IMAC. The letter-number codes represent samples from selected elution fragments, numbered as in figure 10. Protein concentration measurement with the ÄKTA instrument failed in this purification run, so no chromatogram is available.

6.1.4 Avidins

Although several attempts of producing monodin-M2e, rhizavidin-M2e and avidin-M2e were made, no soluble protein could be obtained with the 2-iminobiotin purification method. Because we lacked an efficient production system for these proteins and SpyCatcher-antigen constructs worked well, we moved our focus on them.

6.2 Production of virus-like particles

6.2.1 Creating recombinant baculoviruses

After *E. coli* DH10Bac had been transformed with each pFastBac Dual plasmid, we had to make sure the transposition reactions were successful. After PCR amplification of different DNA stretches in the bacmids (described in Figure 6, p. 30), the sizes of the PCR products were estimated by running them on an agarose gel (Figure 12). Both of our bacmids were of the expected sizes, which were 4246 bp for Spy-VP1 and 5221 bp for the one containing Avi-noro-VP1 and BirA. 200 bp bands were observed in each PCR product made with Tn7L and M13 Reverse competent primers, as expected. The faint ~400 bp bands are likely to derive from the Tn7 primer binding a secondary site in the inserts. 8 bp complementary sequences are identified by a basic local alignment search tool (BLAST) (https://blast.ncbi.nlm.nih.gov/Blast.cgi; 22.3.2018) for both target inserts. The unrelated bacmid used as a positive control produced bands of similar sizes. Thus, our bacmid preparations came from homogenous populations of transformed bacteria.

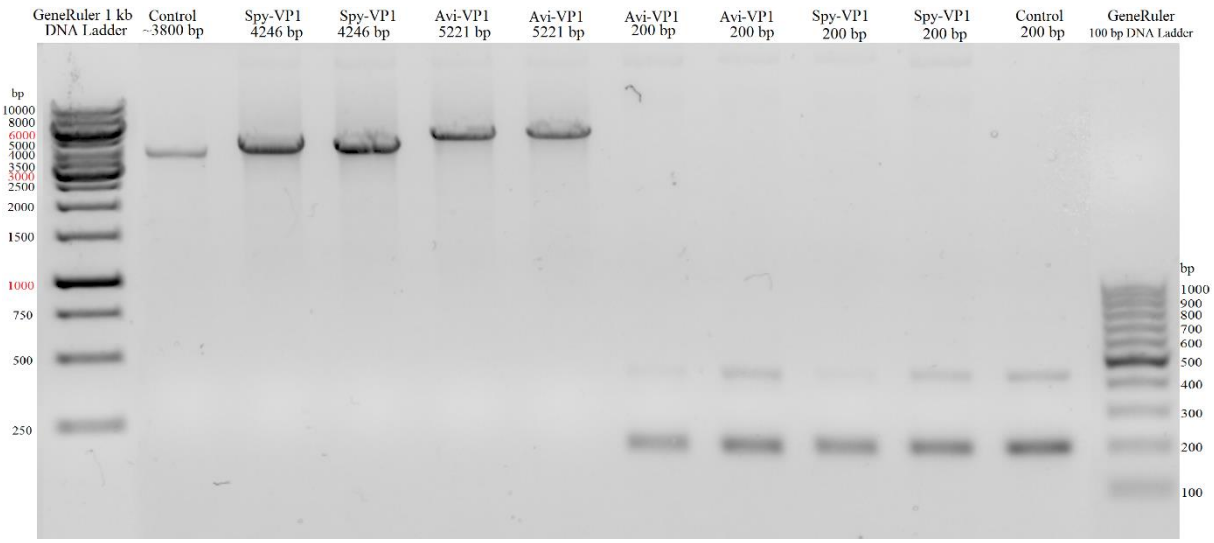

Figure 12. PCR validation of gene transposition. Lanes 2–6 contain bacmids amplified with the M13 Forward and Reverse primers, which amplify the whole transposed expression cassette. Lanes 7–11 contain the same bacmids amplified with the Tn7L and M13 Reverse primers that produce a ~200 bp reaction product with recombinant bacmids and no reaction product with empty bacmids. A recombinant bacmid from another project used as a positive control.

6.2.2 Titration of baculovirus stocks

Infective baculovirus titers of the prepared stocks were measured with BacPAK Baculovirus Rapid Titer Kit and the results are shown in Table 1. Stock solutions with less than 10^8 FFU/mL cannot be used for large-scale protein expression rounds, but P2 stocks can still be amplified further. 50 mL of each of these baculovirus stocks were sufficient for the expression optimization experiments in this project.

Table 1. Titration of recombinant baculovirus stocks. The virus concentrations obtained from BacPAK Baculovirus Rapid Titer Kit are listed here. Three dilutions of each virus preparation were used to infect each well of cells. Only wells with "focus counts" of 5–100 were included, others are named "NA" for not available.

	Dilution			
Virus stock	**10^{-4}**	**10^{-5}**	**10^{-6}**	**Virus Titer (FFU/mL)**
Spy-noro-VP1 P2	2.1E+07	3.5E+07	NA	**2.8E+07**
Avi-noro-VP1 P2	1.2E+07	1.9E+07	NA	**1.5E+07**
WT-noro-VP1 P4	NA	1.0E+08	2.3E+08	**1.7E+08**

6.2.3 Virus-like particle expression

After creating large P2 and P4 stocks of recombinant baculoviruses with high titers, the stocks were used in pilot expression experiments to compare Sf9 and Hi5 cells and using different MOI values for noro-VLP expression efficiency. Most combinations produced a clear double band pattern in SDS-PAGE analysis that ran between the 50 and 70 kDa bands in PageRuler Unstained Broad Range Protein Ladder. This matches the predicted weights of the full-length noro-VLPs (61 kDa for Spy-noro-VLP and for Avi-noro-VLP, 59 kDa for WT-noro-VLP). The molecular weights were estimated with the ProtParam web tool (https://web.expasy.org/protparam/; 26.3.2018) based on the amino acid sequence of each VLP. The double band is due to a natural posttranslational N-terminal truncation of noro-VP1 (more on p. 47) that is expected to reduce protein size by 3.4 kDa. A purified noro-VLP from a different norovirus GII.4 strain (004/95M-14/1995/AU) was added to the gels as a control. According to the SDS-PAGE analyses (Figure 13), Hi5 cells were significantly better at expressing all tested noro-VLPs. The differences between the tested MOI values were small, but values of 1.0 were used in further expression rounds for Spy-noro-VLPs and WT-noro-VLPs and 0.5 for Avi-noro-VLPs.

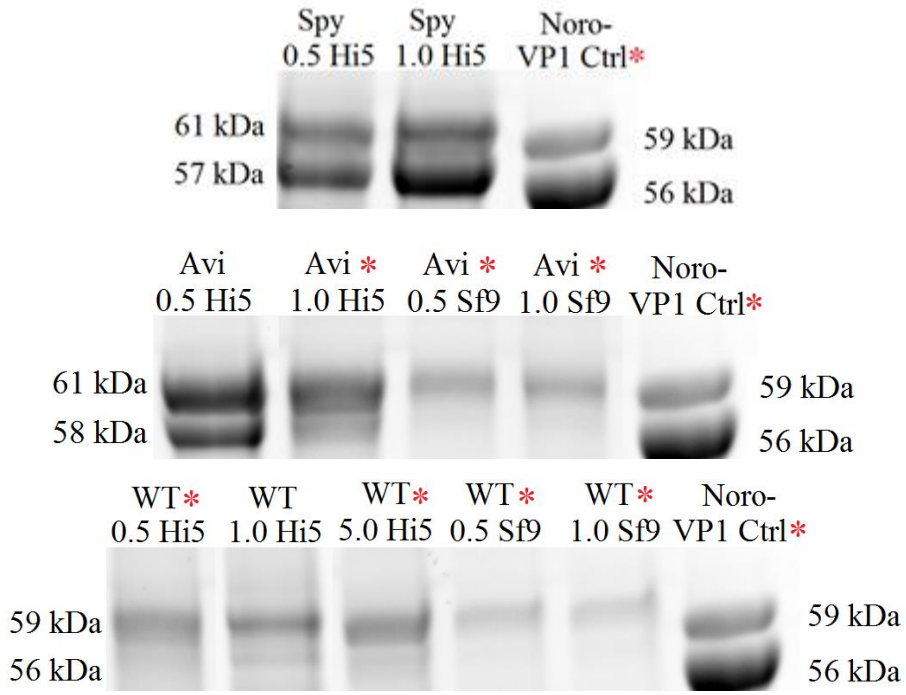

Figure 13. Effects of insect cell line and MOI value on noro-VLP expression. These images show SDS-PAGE results of VLP expression supernatants in the area between 50 and 70 kDa bands in molecular weight markers. The predicted molecular weight of each protein is shown to the left and right of each image. The noro-VLP, MOI value and cell line used are described above each lane (Spy for Spy-noro-VLP, Avi for Avi-noro-VLP and WT for WT-noro-VLP). A purified noro-VP1 protein from a different strain of norovirus GII.4 was used as control. A WB of samples marked with a red asterisk (*) are shown in Figure 15 (p. 43).

6.2.4 Purification of SpyTagged norovirus-like particles

Spy-noro-VLP was purified with a two-step purification process by combining 30% sucrose cushion pelleting and cation exchange chromatography. Samples from checkpoints in the purification process were analyzed together with selected elution fractions using SDS-PAGE. The gel image shows that the protein preparation was considerably pure already after the sucrose cushion pelleting phase (Figure 14B, "LOAD"). Sample "FT" on the same gel shows that a significant proportion of the target proteins failed to bind the resin. The VLP was eluted from the column by a stepwise gradient consisting of 0.1 M, 0.2 M and 0.4 M NaCl. Most of the VLP eluted from the column as a sharp peak (fractions B7 and B6) with 0.4 M NaCl. These fractions contained two additional, faint bands of about 120 kDa in size, but all in all, the elution fractions seemed to contain over 95% Spy-noro-VLP, according to the gel image. Based on absorbance measurements at 280 nm, total noro-VLP yield for this production and purification round was estimated to be roughly 11 mg/L.

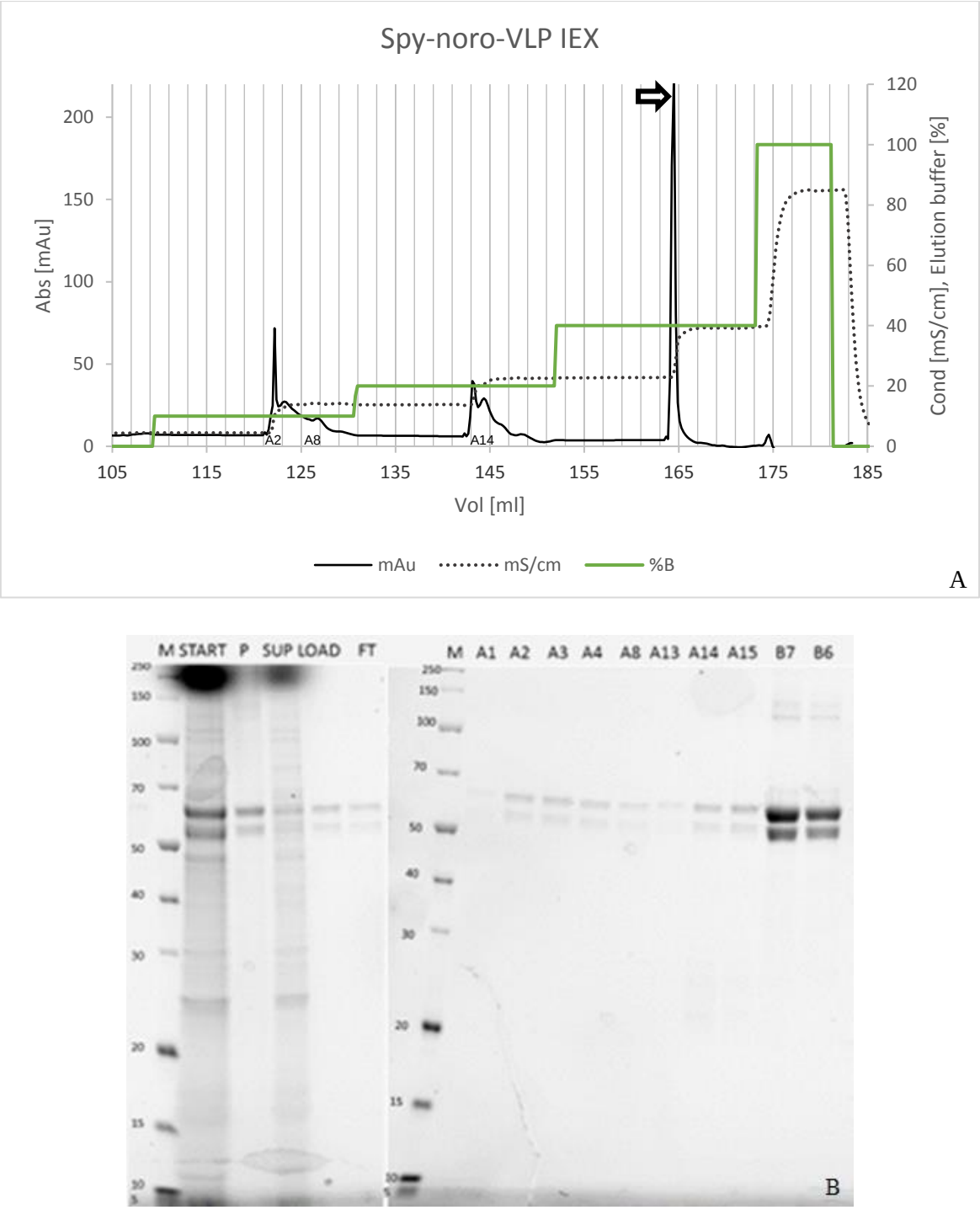

Figure 14. Spy-noro-VLP sucrose cushion and IEX purification. A) A chromatogram of the elution of Spy-noro-VLP. Locations of selected elution fractions are indicated in the figure. Each raise of elution buffer concentration (solid green line) eluted some target protein, as seen from the solid black absorbance (Abs) line, but most of it eluted in fractions B7 and B6, which are around the highest peak (indicated by an arrow). Conductivity (Cond) is shown as a dotted line. B) Stain-free image of purification samples on an SDS-PAGE gel. Lanes labeled M contain PageRuler Unstained Broad Range Protein Ladder. The lane "START" contains a sample of the protein solution before sucrose cushion pelleting. "P" is a sample of the diluted pellet after sucrose pelleting and "SUP" represents the supernatant of the same ultracentrifugation. "LOAD" is a sample of the solution loaded on the chromatography column. Proteins that did not bind the resin are in the "FT" sample. The lanes on the right contain the elution fractions shown in panel A.

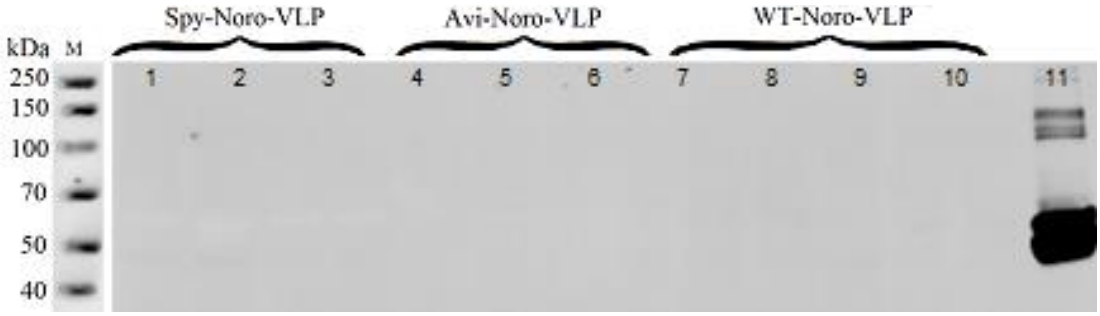

Figure 15. Western blot analysis of noro-VLP samples with an anti-norovirus antibody. Samples of Spy-noro-VLP (lanes 1–3), Avi-noro-VLP (4–6) and WT-noro-VLP (7–10) expression supernatants produced using different MOI values were blotted on the membrane with a purified noro-VLP control (lane 11). Lane M contains PageRuler Unstained Broad Range Protein Ladder, marked in the membrane with a WB marker pen, which can be imaged with a wavelength of 700 nm. Monoclonal mouse anti-norovirus GII.4 antibodies were used for noro-VLP detection and imaged with an anti-mouse antibody that is visible in 800 nm with the Odyssey system. The corresponding Avi-noro-VLP, WT-noro-VLP and control samples are marked with a red asterisk (*) in the Stain-free-imaged gel in Figure 13 (p. 41). The Spy-noro-VLP samples in Figure 13 are from another gel, so the ones in this blot are not shown. They were similar in intensity to the Spy-noro-VLP samples that are shown, though.

6.2.5 Norovirus-specific antibodies were unable to detect recombinant VLPs

We did several WB analyses of our recombinant noro-VLP samples with an anti-norovirus monoclonal antibody, but every time only the independently produced noro-VLP (strain 004/95M-14/1995/AU) used as a positive control was recognized. An example is shown in Figure 15.

6.2.6 Baculoviruses were efficiently removed during noro-VLP purification process

Purified Spy-noro-VLPs were analyzed in WB together with unpurified Avi-noro-VLPs and a baculovirus control. An anti-gp64 antibody specifically recognized the baculovirus control and the unpurified noro-VLP preparations, but did not show staining in the purified samples (Figure 16). This suggests that the purification protocol effectively removes baculoviruses from the preparation.

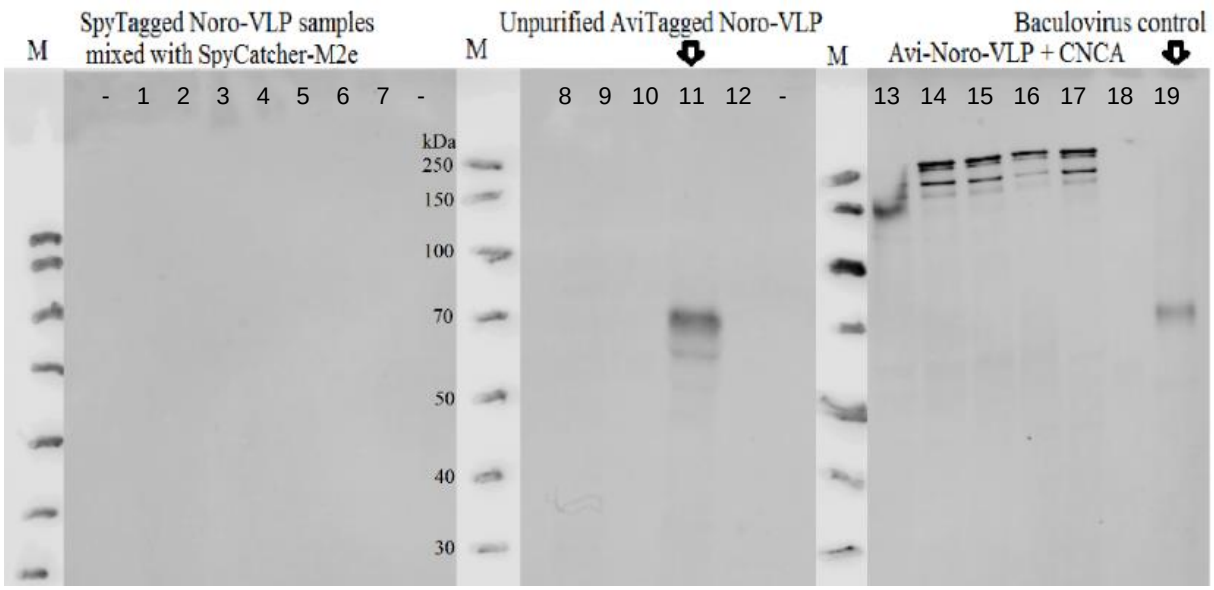

Figure 16. Western blot analysis of noro-VLP samples with an anti-gp64 antibody. The samples on this nitrocellulose membrane are from a conjugation experiment in which purified Spy-noro-VLPs were mixed with SpyCatcher-M2e (lanes 1–7) and unpurified Avi-noro-VLPs with avidin (CNCA) (lanes 13–17). Other lanes: 8&12=Spy-noro-VLP, 9=SpyCatcher-M2e, 10=CNCA, 11=Avi-noro-VLP, 18=Spy-noro-VLP+CNCA. A part of the corresponding gel is shown in Figure 19 (p. 46). The baculovirus control and unpurified Avi-noro-VLPs are stained by the anti-gp64 antibody. They are indicated in the figure by arrows. Lanes 13–17 also contain unpurified Avi-noro-VLP, but these samples were not boiled, so multimeric forms of gp64 are detected. M lanes contain PageRuler Unstained Protein Ladder, marked in the membrane with a WB marker pen. The protein markers were imaged with the Odyssey system using the 700-nm channel and pasted in this figure (imaged with the 800-nm channel).

6.3 SpyCatcher/SpyTag conjugation

In the first attempt at conjugating SpyCatcher-antigens to Spy-noro-VLPs, SDS-PAGE-based band mobility shift analysis (Figure 17) showed that covalent bonds had formed between VP1 proteins and antigens. From the intensity differences of the bands, it can be estimated that approximately half of VP1 proteins were conjugated with SpyCatcher-antigens. However, DLS studies showed that most of the protein in these reaction mixtures had agglomerated. The conjugation was done in a mixture of citrate buffer (pH 5) and phosphate buffer (pH 7.5). In the second attempt, the conjugation was done in PBS and in milder agitation. This time, in addition to seeing the same band mobility shifts in SDS-PAGE, monodisperse particles of around 56 nm were detected with DLS. The average hydrodynamic diameter of undecorated particles in all measurements was 48 nm. Example DLS analyses of an undecorated and decorated Spy-noro-VLP are shown in Figure 17D.

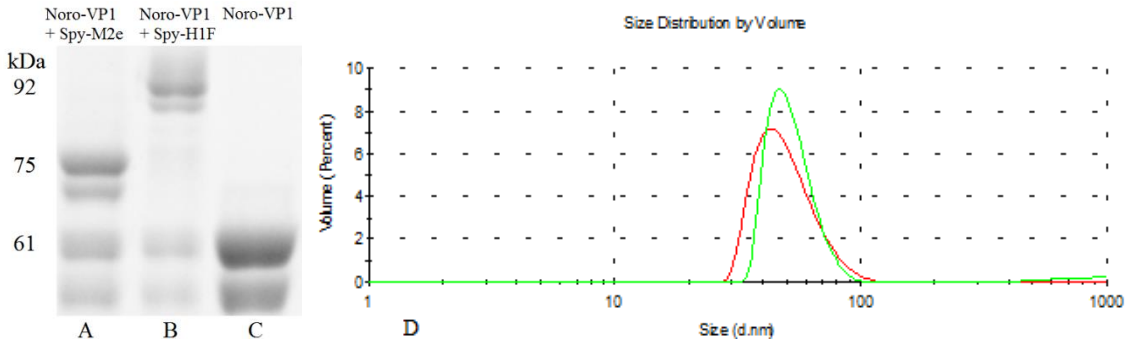

Figure 17. Covalent conjugation between influenza antigens and norovirus VP1 protein via SpyCatcher–SpyTag linkage. Stain-free-imaged SDS-PAGE gel is shown on the left panel. Size estimates of the full-length proteins are shown to the left of the figure. A) Spy-noro-VP1 (61 kDa) mixed with the 15 kDa SpyCatcher-M2e. B) Spy-noro-VP1 mixed with the 31 kDa SpyCatcher-H1F. C) Spy-noro-VP1 alone. D) The size estimate of the reaction product of Spy-noro-VP1 and SpyCatcher-M2e is shown in green (peak at 52 nm). A non-conjugated noro-VLP particle is shown in red (peak at 50 nm).

6.4 Avidin binding studies with AviTagged norovirus-like particles

Biotinylation of Avi-noro-VLPs was tested in two separate assays. The WB-based analysis showed that avidin binds Avi-noro-VP1 proteins that are separated on an SDS-PAGE gel and blotted onto a membrane (Figure 18). Spy-noro-VP1 proteins were not bound by avidin. The CNCA (1 µg/well) that was in the gel as a positive control was not detected by the anti-avidin antibody, but this is most likely due to some technicality like the protein missing the membrane when blotting. Biotinylated BSA (1 µg/well) was bound by avidin and detected.

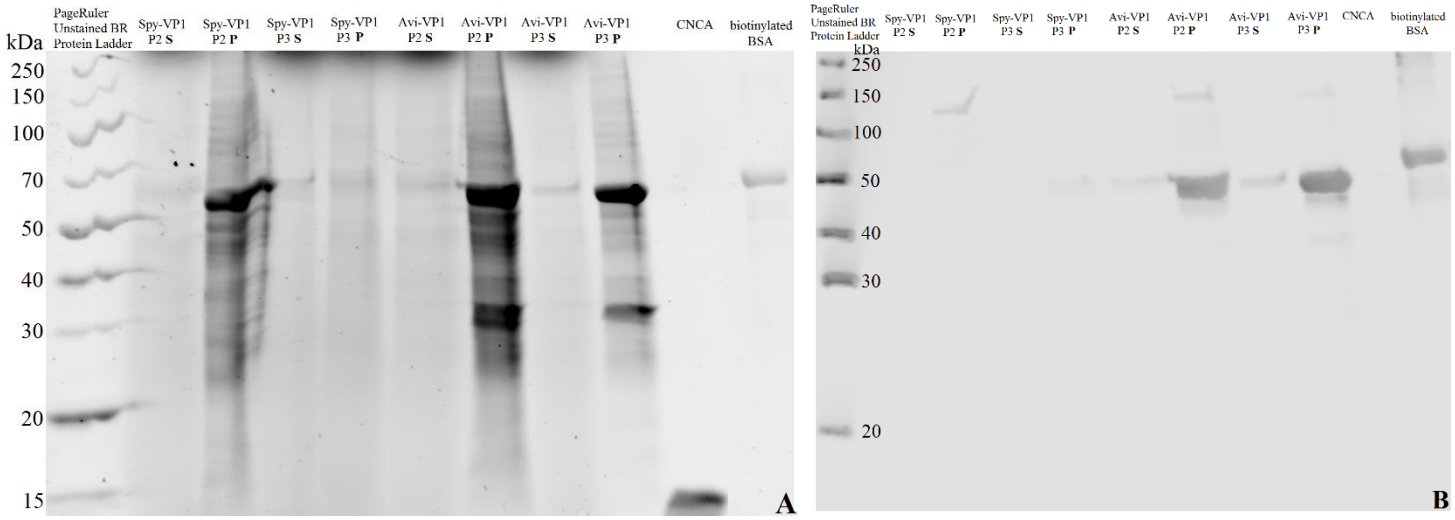

Figure 18. SDS-PAGE and western blot showing the biotinylation of Avi-noro-VP1 proteins. The Stain-free-imaged gel in panel A was blotted onto a membrane, shown in panel B. Pellet (**P**) and supernatant (**S**) samples of Avi-noro-VP1 and Spy-noro-VP1 baculovirus stocks were run on the gel. After blocking with BSA, the membrane was incubated in neutralized chimeric avidin (10 µg/mL) and then with a primary anti-avidin antibody and a secondary antibody that can be imaged with a wavelength of 700 nm with the Odyssey system. The protein ladder was marked in the membrane with a WB marker pen, which is imaged with the same wavelength.

When unpurified supernatants of Avi-noro-VLPs were mixed together with increasing amounts of CNCA and analyzed with SDS-PAGE in conditions that support the tetrameric form of avidin, the distance covered by AviTagged VP1 proteins in the gel decreases with increasing CNCA amounts (Figure *19*). In these conditions, avidin tetramers mostly keep intact and able to bind biotin, but penetration of the globular, tetrameric protein through the gel is unpredictable. The theoretical molecular weight of the CNCA tetramer is ~57 kDa. VLPs, on the other hand, should denature to their subunits efficiently. In the well with the highest amount of CNCA, the bands become very blurred. A similar amount of CNCA also seems to affect the drift of SpyTagged VP1, but in a slightly different way.

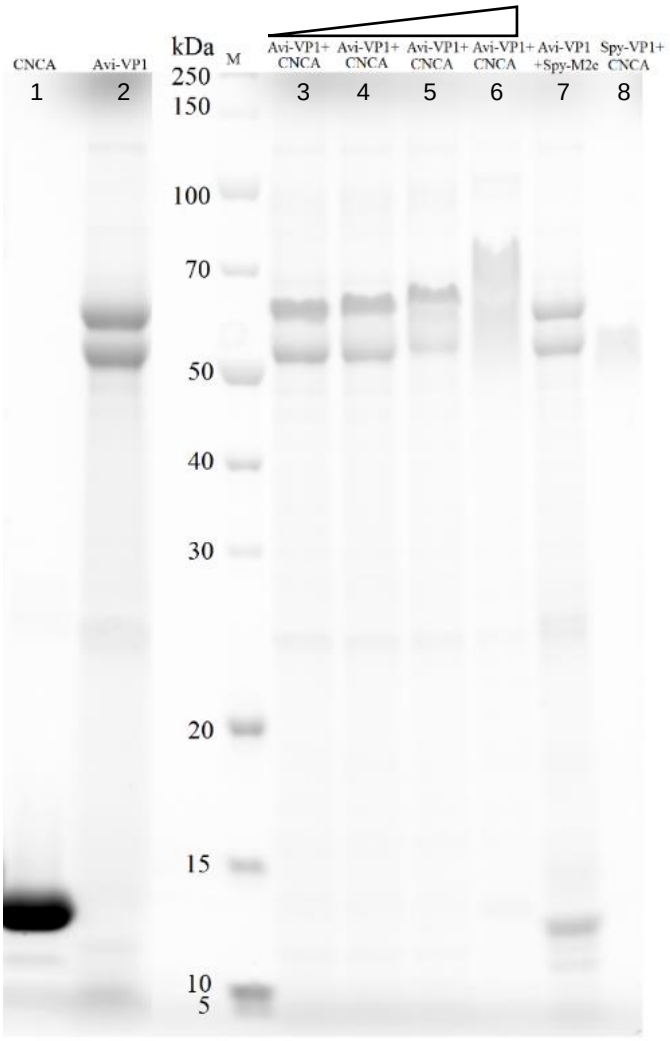

Figure 19 A Stain-free image of SDS-PAGE analysis of avidin mixed with Avi-noro-VLP. Samples 3–8 were mixed with SDS-PAGE sample buffer and warmed in 60 °C for 10 minutes before electrophoresis, the others boiled in SDS-PAGE sample buffer, as usual. On lane "M" is the PageRuler Unstained Protein Ladder. CNCA concentration rises in the conjugation samples 3–6 from left to right. It was added in the wells as follows: 1) 12 µg, 3) 1.2 µg, 4) 2.4 µg, 5) 6 µg, 6) 8 µg, 8) 4.8 µg.

7 Discussion

SDS-PAGE analysis of noro-VP1 samples showed a double band pattern of approximately 60 kDa proteins. This matches the predicted molecular weights of the full-length proteins well. The double band pattern is typical for norovirus VP1 and is due to a posttranslational cleavage of a 34-amino-acid-long (3.4 kDa) N-terminal fragment of the protein [56]. Both protein forms probably participate in the assembly of the viral capsid [76]. It is worth noting that expression of a truncated form of noro-VP1 with an N-terminal deletion of the first 34 amino acids resulted in low expression levels and no virus-like particles at all [77]. This suggests that at least some levels of full-length noro-VP1 are needed for either correct VP1 folding or for VLP assembly. No study that would prevent the N-terminal cleavage from happening altogether has yet been reported, so the importance of N-terminally truncated noro-VP1 in the assembly of the norovirus capsid remains to be solved.

An effective antibody would have been useful in the identification of the produced noro-VLPs in WB. The one we had was a mouse monoclonal antibody raised against norovirus GII.4 strain Hu/NLV/GII/MD145-12/1987/US (GenBank ID: AY032605). The noro-VLP used as a positive control in the studies was of strain GII.4 004/95M-14/1995/AU, and SpyTagged, AviTagged and WT-noro-VLP are all Hu/GII.4/Sydney/NSW0514/2012/AU. The P domain of norovirus capsid contains most of its antibody epitopes [78]. According to protein BLAST, the P domain of our control noro-VLP has a sequence similarity of 96% with the antibody-inducing strain, while the corresponding value is only 88% with the target proteins of this study. The differences are large enough to explain the total lack of recognition for the target proteins in WB analyses. In further studies, a norovirus GII.4 Sydney specific antibody would help identify the expressed noro-VLPs. An anti-SpyCatcher antibody would also allow more sensitive identification of SpyCatcher-antigen fusion proteins. Nevertheless, the undecorated particles observed in DLS studies were approximately 48 nm in diameter, which is close to the 42 nm measured in previous studies of HisTagged noro-VLPs [53]. Together with the success in conjugation studies, the identity of the produced proteins is clear even without specific antibodies. If further validation of the produced proteins is needed, proteomics methods could be used.

A rough estimate of noro-VLP production yields was put at 11 mg/L, based on concentration measurements of the single purified 50-mL batch. A lot of VP1 protein is lost during purifications, as can be seen from the pellet and flow-through samples of Figure 14B (p.42). Koho et. al [76] describe a yield of 100 mg/L for wild type noro-VLPs purified by polyethylene glycol (PEG) precipitation and sucrose gradient filtering. On the other hand, IMAC purification of HisTagged noro-VLPs yielded only 1.5 mg/L of [53]. Even though it seems to have been successful in the purification of wild-type noro-VLPs, PEG precipitation may not be the best of strategies in vaccine production, because PEG may mask the surfaces of VLPs [53]. This might, in turn, interfere with the conjugation of SpyTag. In summary, the yield of Spy-noro-VLP obtained after purification is already relatively good, but it is still possible to improve it by considering the purification steps necessary to obtain the desired purity levels. The ultracentrifugation step in this vaccine manufacture protocol can be problematic later on, because it is not easily scaled up to an industrial scale. Avi-noro-VLP or WT-noro-VLP were not purified, but there is no reason why the same IEX purification protocol would not work for them with similar levels of success, since they only differ by their small C-terminal tags.

Minor impurities of ~30 kDa were observed in the purification of SpyCatcher-M2e (Figure 10B, p. 37). By size, this could well be a dimer of SpyCatcher-M2e. The fact that the amounts of the impurities seem to correlate with the amounts of SpyCatcher-M2e in the lanes supports this hypothesis. A similar phenomenon can be seen in the corresponding gel image for Spy-noro-VLP (Figure 14B, p. 42). Here, approximately 120 kDa bands appear only in the wells with the highest amounts of Spy-noro-VP1 protein. They cannot be seen in the "Load" sample either, so this is a strong indication of the VP1 remaining partially in a dimeric form even after boiling, when its concentration is large enough. As mentioned in Chapter 3.4, VP1 acts as a dimer when forming the VLP, so finding dimers in the gel is not entirely unexpected.

According to WB analysis with anti-gp64 antibodies, the purified Spy-noro-VLP samples do not contain baculoviruses after IEX purification. This is well in line with earlier observations on noro-VLP purification [76]. The same publication reported gp64 signal to be still present after a similar sucrose filtration purification step, which most likely applies for our purification process as well (not analyzed). Baculoviruses are known to

be safe for vertebrate [13] cells, and have been found to even work efficiently as adjuvants in similar vaccine preparations [79]. Even if their use as adjuvants in human vaccines would be approved, though, it is likely that the levels of baculoviruses need to be controlled carefully, so their initial removal is important. Bacterial endotoxins are another matter to consider when producing vaccine components in *E. coli*, but this was not measured in this work. Modifying the purification protocol according to measured endotoxin levels may still be required for the antigens produced in bacteria, since a single-step IMAC purification process does not always lower the endotoxin content to approvable levels [76].

In further studies, it may be worthwhile to study if the efficient SpyCatcher conjugation reaction could be utilized in the purification of Spy-noro-VLPs. One approach would be to mix the unpurified Spy-noro-VLP-containing supernatant to SpyCatcher-antigen fusion proteins. Then, successfully decorated VLPs can be purified from the mixture with IMAC by utilizing the HisTag in the N-terminus of SpyCatcher-antigens. If SpyCatcher conjugation is efficient even in this protein-rich solution, purification steps can be significantly reduced. Recent proof of *in vivo* conjugation via the SpyCatcher/SpyTag system supports this hypothesis [80]. It might even be possible to simply mix the bacterial supernatant that contains SpyCatcher-antigens with the Spy-noro-VLP-containing insect supernatant and purify the decorated VLPs in a single step. If effective, this alternative manufacture protocol could be used to speed up vaccine production and reduce costs when large quantities of a single vaccine type are needed, for example when fighting a rampant pandemic.

Next, the produced vaccine compounds of M2e- and H1F-decorated Spy-noro-VLPs should be compared to free M2e and H1F regarding their immunogenicity. Should these pre-clinical vaccine experiments yield promising results even when compared to current vaccine solutions, the next phase in influenza vaccine development would be to move to clinical studies. If the platform proves functional still in the pre-clinical studies, it should also be tested with antigens from other pathogens and maybe even self-antigens.

It is likely that the relatively large (15 kDa) SpyCatcher does not form stable proteins with all fusion partners. It might also prove harmfully immunodominant in some vaccine approaches. Fortunately, the Spy-noro-VLP platform should be compatible with

a related system that requires only a small peptide tag in both vaccine components for bioconjugation. Fierer et al. [81] developed a system where the CnaB protein was split into three parts, instead of two as in SpyCatcher. Here, two β-strands have been separated from the protein: the one containing the reactive aspartic acid (SpyTag) and the one that contains the reactive lysine, called KTag. When proteins tagged with SpyTag and KTag are mixed together, they fuse enzymatically via an isopeptide bond in the presence of the rest of the protein, termed SpyLigase. Therefore, with future antigens designed for this vaccine platform, the 15 kDa SpyCatcher protein can be replaced with the 10-amino-acid peptide called KTag.

In the clinical phase, commercial viewpoints of the vaccine candidates should be considered. The inventors of SpyCatcher/SpyTag technology have protected its commercial use with patents that are valid in Europe and in USA (https://patents.google.com/patent/WO2011098772A1/en; 1.4.2018). They have also started a company that seeks to commercialize new vaccine platforms with the technology (http://www.spybiotech.com; 1.4.2018). For any commercial use of the Spy-noro-VLP vaccine platform, a licensing agreement or a partnership may have to be formed with the patent holders. Patent applications for the H1F antigen have been filed in Europe and USA (https://patents.google.com/patent/EP3137487A1; 1.4.2018). Avi-noro-VLPs were successfully formed and biotinylated, so an efficient system to create avidin-antigens would be sufficient to create a vaccine platform without such intellectual property rights issues. Even though some avidin forms have been patented in the past, there are several unpatented ones available for use. Patent applications for AviTag have been filed, but they were withdrawn in 2006 (https://patents.google.com/patent/WO2004076670; 9.4.2018).

Although it has been over 70 years since the first influenza vaccine was distributed, the same egg-based manufacture technology is still in use. However, there is much research that aims for new vaccine technologies, lot of which is directed expressly to recombinant protein vaccines. The way has already been paved for the coming of recombinant influenza vaccines by Flublok (Sanofi Pasteur, Lyon, France), which was approved for commercial use in the USA in 2013. Flublok is comprised of full-length, wild-type HA protein that is recombinantly expressed with the baculovirus expression system in insect

cells. Such a vaccine does not provide any broader immunity than conventional, egg-based influenza vaccines, but the generation of a new vaccine with recombinant technology can be done significantly faster. [82]

Flublok is a step to the right direction, but it still falls far from the goal of a universal influenza vaccine. With this in mind, recombinant vaccines containing peptides from M2e and HA stem have been studied a lot recently. The group that engineered the H1F antigen tested its immunogenicity when injected together with a similar antigen from an H5 influenza strain. The vaccine protected mice from influenza strains H1, H3 and H5, which was the broadest protective effect reported so far [12]. Alas, further studies by the group showed that in ferrets, similar ministem vaccines lacked efficacy [83]. They concluded that these promising vaccine candidates need to be "enhanced" to be effective in larger, outbred species (like humans). Displaying antigens on VLPs usually boosts their immunogenicity, so the design used in thesis work is a potential solution to the problem.

M2e is a very conserved influenza antigen and an attractive candidate for a universal vaccine, but it is not very immunogenic by itself. To make an efficient M2e vaccine, M2e has been displayed on numerous VLPs, some of which have already advanced to clinical trials, as mentioned in Chapter 3.1.3. Studies have shown that even VLP-linked M2e vaccines work better when M2e is displayed together with other influenza antigens or in tandem repeats [6]. An interesting strategy that could be easily adapted to the Spy-noro-VLP platform is to incorporate four slightly different M2e fragments from human, avian and swine influenza species onto a single influenza M1 VLP. Such a vaccine granted effective and broad protection to mice in pre-clinical studies [84].

A very similar approach to creating a modular vaccine platform was reported by Brune et al. [13]. They genetically fused SpyCatcher to the capsid protein of the bacteriophage AP205 and produced functional VLPs in *E. coli*. The HisTagged VLPs were purified with IMAC. The group also produced SpyTagged malaria antigens and cancer-related self-antigens in *E. coli*. The produced VLPs and antigens were conjugated successfully and the conjugated malaria-VLPs generated a stronger immune response in mice when compared to unconjugated controls. In this approach, the VLPs and antigens were both produced in *E. coli*, which requires strict control of endotoxin levels. Brune et al.

managed to lower them down to acceptable levels in the case of VLPs (endotoxin levels in antigen preparations not reported) by using an *E. coli* strain engineered to produce less endotoxins and by using additional washing steps with Triton X-114. Compared to the Spy-noro-VLP platform, the AP205-VLPs may be slightly simpler to produce as they do not require insect cell systems, but as yields are not reported in the article, production efficiencies are difficult to compare at this point. In the end, broad applicability and the immunogenicity of the platform are more important properties than pure production values.

In recent years, a lot of progress has been made in the direction of making better influenza vaccines. Hunting for a universally protecting vaccine formula this actively will most likely result in finding one at some point. However, this is not likely to stop the need for new vaccine formulae altogether. The fact that some regions in the influenza genome have remained conserved until now does not necessarily mean that they will in the future. In fact, widespread vaccination that targets these regions may well facilitate the birth of escape mutants with increased variance in the conserved areas. Yet, the virus is not as equipped to mutate these areas as the HA head domain, so their evolution should slow down. The production rates of modular, recombinant vaccines made e.g. with the Spy-noro-VLP platform should be enough to match the moderated evolution rate of influenza with ease.

8 Conclusions

Spy-noro-VLPs, Avi-noro-VLPs and WT-noro-VLPs were efficiently expressed in insect cells. Hi5 cells were significantly more efficient in producing all VLPs, as compared to Sf9 cells. An optimal MOI value for the expression of each noro-VLP was found. However, the expression levels were high with each MOI value tested. A 50-mL batch production of Spy-noro-VLP was purified successfully with sucrose cushion pelleting combined to cation exchange chromatography. The yield of >95% pure Spy-noro-VLP was estimated to be 11 mg/L. No other kinds of noro-VLPs were purified, but the same protocol should yield similar results with the near-identical VLPs.

Since detectable amounts of soluble avidin-antigen fusion proteins could not be obtained regardless of several attempts, most of antigen fusion protein production efforts were directed to SpyCatcher proteins. Expression of both SpyCatcher-fused M2e and H1F was efficient in *E. coli*. 500-mL batch productions of SpyCatcher-M2e and SpyCatcher-H1F were done with the optimal *E. coli* strain, induction parameters and expression temperature and purified with IMAC. Yields for >95% pure SpyCatcher-M2e and SpyCatcher-H1F were 34 and 27 mg/L, respectively.

SDS-PAGE and Western blotting analyses showed that the produced Avi-noro-VLPs were effectively biotinylated when co-expressed with BirA in insect cells. Dialyzed and purified Spy-noro-VLPs were mixed with SpyCatcher-M2e and SpyCatcher-H1F and antigen-decorated, monodisperse Spy-noro-VLPs were obtained. Covalent conjugation of SpyCatcher-antigens and Spy-noro-VLPs was observed with band mobility shift analyses. The next logical step in future studies would be to formulate vaccines out of M2e- and H1F-decorated Spy-noro-VLPs and compare their immunogenicity to free M2e and H1F in an animal model.

9 References

[1]Kang SM, Kim MC, Compans RW. Virus-like particles as universal influenza vaccines. *Expert Rev Vaccines* 2012;11(8):995-1007.

[2]Karlsson Hedestam GB, Fouchier RA, Phogat S, Burton DR, Sodroski J, Wyatt RT. The challenges of eliciting neutralizing antibodies to HIV-1 and to influenza virus. *Nat Rev Microbiol* 2008;6(2):143-155.

[3]Szewczyk B, Bienkowska-Szewczyk K, Krol E. Introduction to molecular biology of influenza A viruses. *Acta Biochim Pol* 2014;61(3):397-401.

[4]The College of Physicians of Philadelphia. Influenza. Philadelphia, USA; 2018.

[5]Nachbagauer R, Krammer F. Universal influenza virus vaccines and therapeutic antibodies. *Clin Microbiol Infect* 2017;23(4):222-228.

[6]Deng L, Cho KJ, Fiers W, Saelens X. M2e-Based Universal Influenza A Vaccines. *Vaccines (Basel)* 2015;3(1):105-136.

[7]Medina RA, Garcia-Sastre A. Influenza A viruses: new research developments. *Nat Rev Microbiol* 2011;9(8):590-603.

[8]Centers for Disease Control and Prevention (CDC). The 2009 H1N1 Pandemic: Summary Highlights, April 2009-April 2010. 2010.

[9]Rossman JS, Lamb RA. Influenza virus assembly and budding. *Virology* 2011;411(2):229-236.

[10]Centers for Disease Control and Prevention (CDC). Frequently Asked Flu Questions 2017-2018 Influenza Season. 2018.

[11]Ebrahimi SM, Tebianian M. Influenza A viruses: why focusing on M2e-based universal vaccines. *Virus Genes* 2011;42(1):1-8.

[12]Valkenburg SA, Mallajosyula VV, Li OT, Chin AW, Carnell G, Temperton N, et al. Stalking influenza by vaccination with pre-fusion headless HA mini-stem. *Sci Rep* 2016;6:22666.

[13]Brune KD, Leneghan DB, Brian IJ, Ishizuka AS, Bachmann MF, Draper SJ, et al. Plug-and-Display: decoration of Virus-Like Particles via isopeptide bonds for modular immunization. *Sci Rep* 2016;6:19234.

[14]Leblanc P, Moise L, Luza C, Chantaralawan K, Lezeau L, Yuan J, et al. VaxCelerate II: rapid development of a self-assembling vaccine for Lassa fever. *Hum Vaccin Immunother* 2014;10(10):3022-3038.

[15]Centers for Disease Control and Prevention (CDC). Types of Influenza Viruses. 2017.

[16]Kumlin U, Olofsson S, Dimock K, Arnberg N. Sialic acid tissue distribution and influenza virus tropism. *Influenza Other Respir Viruses* 2008;2(5):147-154.

[17]Nelson DL, Cox M, M. Lehninger Principles of Biochemistry. 3rd ed. New York, USA*: Worth Publishers*; 2000.

[18]Russell RJ, Kerry PS, Stevens DJ, Steinhauer DA, Martin SR, Gamblin SJ, et al. Structure of influenza hemagglutinin in complex with an inhibitor of membrane fusion. *Proc Natl Acad Sci U S A* 2008;105(46):17736-17741.

[19]Chen BJ, Leser GP, Jackson D, Lamb RA. The influenza virus M2 protein cytoplasmic tail interacts with the M1 protein and influences virus assembly at the site of virus budding. *J Virol* 2008;82(20):10059-10070.

[20]Cheung TK, Guan Y, Ng SS, Chen H, Wong CH, Peiris JS, et al. Generation of recombinant influenza A virus without M2 ion-channel protein by introduction of a point mutation at the 5' end of the viral intron. *J Gen Virol* 2005;86(Pt 5):1447-1454.

[21]Bommakanti G, Citron MP, Hepler RW, Callahan C, Heidecker GJ, Najar TA, et al. Design of an HA2-based Escherichia coli expressed influenza immunogen that protects mice from pathogenic challenge. *Proc Natl Acad Sci U S A* 2010;107(31):13701-13706.

[22]Corti D, Voss J, Gamblin SJ, Codoni G, Macagno A, Jarrossay D, et al. A neutralizing antibody selected from plasma cells that binds to group 1 and group 2 influenza A hemagglutinins. *Science* 2011;333(6044):850-856.

[23]Chen J, Wharton SA, Weissenhorn W, Calder LJ, Hughson FM, Skehel JJ, et al. A soluble domain of the membrane-anchoring chain of influenza virus hemagglutinin (HA2) folds in Escherichia coli into the low-pH-induced conformation. *Proc Natl Acad Sci U S A* 1995;92(26):12205-12209.

[24]Mallajosyula VV, Citron M, Ferrara F, Lu X, Callahan C, Heidecker GJ, et al. Influenza hemagglutinin stem-fragment immunogen elicits broadly neutralizing antibodies and confers heterologous protection. *Proc Natl Acad Sci U S A* 2014;111(25):E2514-23.

[25]Neirynck S, Deroo T, Saelens X, Vanlandschoot P, Jou WM, Fiers W. A universal influenza A vaccine based on the extracellular domain of the M2 protein. *Nat Med* 1999;5(10):1157-1163.

[26]Qin G, Yu K, Shi T, Luo C, Li G, Zhu W, et al. How does influenza virus A escape from amantadine? *J Phys Chem B* 2010;114(25):8487-8493.

[27]Liu W, Zou P, Ding J, Lu Y, Chen Y. Sequence comparison between the extracellular domain of M2 protein human and avian influenza A virus provides new information for bivalent influenza vaccine design. *Microbes and Infection* 2005;7(2):171-177.

[28]Laitinen OH, Nordlund HR, Hytonen VP, Kulomaa MS. Brave new (strept)avidins in biotechnology. *Trends Biotechnol* 2007;25(6):269-277.

[29]Wilchek M, Bayer EA, Livnah O. Essentials of biorecognition: the (strept)avidin-biotin system as a model for protein-protein and protein-ligand interaction. *Immunol Lett* 2006;103(1):27-32.

[30]Fairhead M, Howarth M. Site-specific biotinylation of purified proteins using BirA. *Methods Mol Biol* 2015;1266:171-184.

[31]Laitinen OH, Hytonen VP, Nordlund HR, Kulomaa MS. Genetically engineered avidins and streptavidins. *Cell Mol Life Sci* 2006;63(24):2992-3017.

[32]Graslund S, Savitsky P, Muller-Knapp S. In Vivo Biotinylation of Antigens in E. coli. *Methods Mol Biol* 2017;1586:337-344.

[33]Jain A, Cheng K. The principles and applications of avidin-based nanoparticles in drug delivery and diagnosis. *J Control Release* 2017;245:27-40.

[34]Hytonen VP, Maatta JA, Nyholm TK, Livnah O, Eisenberg-Domovich Y, Hyre D, et al. Design and construction of highly stable, protease-resistant chimeric avidins. *J Biol Chem* 2005;280(11):10228-10233.

[35]Pardridge WM. Drug transport across the blood-brain barrier. *J Cereb Blood Flow Metab* 2012;32(11):1959-1972.

[36]Zauner D, Taskinen B, Eichinger D, Flattinger C, Ruttmann B, Knoglinger C, Traxler L, Ebner A, Gruber HJ, Hytönen VP. Regenerative biosensor chips based on switchable mutants of avidin—A systematic study. *Sensors and Actuators B: Chemical* 2016;229:646-654.

[37]Taskinen B, Zauner D, Lehtonen SI, Koskinen M, Thomson C, Kahkonen N, et al. Switchavidin: reversible biotin-avidin-biotin bridges with high affinity and specificity. *Bioconjug Chem* 2014;25(12):2233-2243.

[38]Helppolainen SH, Nurminen KP, Maatta JA, Halling KK, Slotte JP, Huhtala T, et al. Rhizavidin from Rhizobium etli: the first natural dimer in the avidin protein family. *Biochem J* 2007;405(3):397-405.

[39]Lee JM, Kim JA, Yen TC, Lee IH, Ahn B, Lee Y, et al. A Rhizavidin Monomer with Nearly Multimeric Avidin-Like Binding Stability Against Biotin Conjugates. *Angew Chem Int Ed Engl* 2016;55(10):3393-3397.

[40]Laitinen OH, Nordlund HR, Hytonen VP, Uotila ST, Marttila AT, Savolainen J, et al. Rational design of an active avidin monomer. *J Biol Chem* 2003;278(6):4010-4014.

[41]Veggiani G, Zakeri B, Howarth M. Superglue from bacteria: unbreakable bridges for protein nanotechnology. *Trends Biotechnol* 2014;32(10):506-512.

[42]Kang HJ, Coulibaly F, Clow F, Proft T, Baker EN. Stabilizing isopeptide bonds revealed in gram-positive bacterial pilus structure. *Science* 2007;318(5856):1625-1628.

[43]Zakeri B, Fierer JO, Celik E, Chittock EC, Schwarz-Linek U, Moy VT, et al. Peptide tag forming a rapid covalent bond to a protein, through engineering a bacterial adhesin. *Proc Natl Acad Sci U S A* 2012;109(12):E690-7.

[44]Li L, Fierer JO, Rapoport TA, Howarth M. Structural analysis and optimization of the covalent association between SpyCatcher and a peptide Tag. *J Mol Biol* 2014;426(2):309-317.

[45]Quan FS, Lee YT, Kim KH, Kim MC, Kang SM. Progress in developing virus-like particle influenza vaccines. *Expert Rev Vaccines* 2016;15(10):1281-1293.

[46]Bayer ME, Blumberg BS, Werner B. Particles associated with Australia antigen in the sera of patients with leukaemia, Down's Syndrome and hepatitis. *Nature* 1968;218(5146):1057-1059.

[47]Ding X, Liu D, Booth G, Gao W, Lu Y. Virus-Like Particle Engineering: From Rational Design to Versatile Applications. *Biotechnology Journal* 2018.

[48]Mohsen MO, Zha L, Cabral-Miranda G, Bachmann MF. Major findings and recent advances in virus–like particle (VLP)-based vaccines. *Seminars in Immunology* 2017.

[49]Yang M, Lai H, Sun H, Chen Q. Virus-like particles that display Zika virus envelope protein domain III induce potent neutralizing immune responses in mice. *Sci Rep* 2017;7(1):7679-017-08247-9.

[50]Cervarix®. Prescribing information. GlaxoSmithKline, July 2011.

[51]Huhti L, Hemming-Harlo M, Vesikari T. Norovirus detection from sera of young children with acute norovirus gastroenteritis. *J Clin Virol* 2016;79:6-9.

[52]Koho T, Mantyla T, Laurinmaki P, Huhti L, Butcher SJ, Vesikari T, et al. Purification of norovirus-like particles (VLPs) by ion exchange chromatography. *J Virol Methods* 2012;181(1):6-11.

[53]Koho T, Ihalainen TO, Stark M, Uusi-Kerttula H, Wieneke R, Rahikainen R, et al. His-tagged norovirus-like particles: A versatile platform for cellular delivery and surface display. *Eur J Pharm Biopharm* 2015;96:22-31.

[54]Jones MK, Grau KR, Costantini V, Kolawole AO, de Graaf M, Freiden P, et al. Human norovirus culture in B cells. *Nat Protoc* 2015;10(12):1939-1947.

[55]Prasad BV, Hardy ME, Dokland T, Bella J, Rossmann MG, Estes MK. X-ray crystallographic structure of the Norwalk virus capsid. *Science* 1999;286(5438):287-290.

[56]White LJ, Hardy ME, Estes MK. Biochemical characterization of a smaller form of recombinant Norwalk virus capsids assembled in insect cells. *J Virol* 1997;71(10):8066-8072.

[57]Atmar RL, Bernstein DI, Harro CD, Al-Ibrahim M, Chen WH, Ferreira J, et al. Norovirus Vaccine against Experimental Human Norwalk Virus Illness. *N Engl J Med* 2011;365(23):2178-2187.

[58]Blazevic V, Malm M, Arinobu D, Lappalainen S, Vesikari T. Rotavirus capsid VP6 protein acts as an adjuvant in vivo for norovirus virus-like particles in a combination vaccine. *Human Vaccines & Immunotherapeutics* 2016;12(3):740-748.

[59]Lucero Y, Vidal R, O'Ryan GM. Norovirus vaccines under development. *Vaccine* 2017.

[60]Oswald N. What's the problem with ampicillin selection? 2015; Available at: https://bitesizebio.com/25299/whats-the-problem-with-ampicillin-selection-2/. Accessed 4/5, 2018.

[61]Epicentre. EasyLyse bacterial protein extraction solution. 2012; Available at: http://www.epibio.com/docs/default-source/protocols/easylyse-bacterial-protein-extraction-solution.pdf?sfvrsn=8. Accessed 4/6, 2018.

[62]Huhti L, Blazevic V, Puustinen L, Hemming M, Salminen M, Vesikari T. Genetic analyses of norovirus GII.4 variants in Finnish children from 1998 to 2013. *Infect Genet Evol* 2014;26:65-71.

[63]Invitrogen. Bac-to-Bac Baculovirus Expression System User guide. 2015.

[64]Oxford Expression Technologies. baculoFECTIN II USER GUIDE. 2015.

[65]Clontech. BacPAK™ Baculovirus Rapid Titer Kit User Manual. 2011.

[66]Stemcell Technologies. Protocol for Producing Monoclonal Cell Lines Using ClonaCell™ FLEX Semi-Solid Medium. 2012.

[67]Ray S, Steven RT, Green FM, Hook F, Taskinen B, Hytonen VP, et al. Neutralized chimeric avidin binding at a reference biosensor surface. *Langmuir* 2015;31(6):1921-1930.

[68]Bio-Rad. Stainfree imaging technology. 2016; Available at: http://www.bio-rad.com/en-fi/applications-technologies/stain-free-imaging-technology?ID=NZ0G1815. Accessed 4/5, 2018.

[69]Bornhorst JA, Falke JJ. 16] Purification of Proteins Using Polyhistidine Affinity Tags. *Methods Enzymol* 2000;326:245-254.

[70]Thermo Fisher Scientific. Ion exchange chromatography. 2007; Available at: https://tools.thermofisher.com/content/sfs/brochures/TR0062-Ion-exchange-chrom.pdf. Accessed 4/5, 2018.

[71]Lorber B, Fischer F, Bailly M, Roy H, Kern D. Protein analysis by dynamic light scattering: methods and techniques for students. *Biochem Mol Biol Educ* 2012;40(6):372-382.

[72]Hytonen V, Laitinen O, Airenne T, Kidron H, Meltola N, Porkka E, et al. Efficient production of active chicken avidin using a bacterial signal peptide in Escherichia coli. *Biochem J* 2004;384:385-390.

[73]Zhang WB, Sun F, Tirrell DA, Arnold FH. Controlling macromolecular topology with genetically encoded SpyTag-SpyCatcher chemistry. *J Am Chem Soc* 2013;135(37):13988-13997.

[74]Schrödinger L. The PyMOL Molecular Graphics System, Version 2.0.6. 2015.

[75]Guex N, Peitsch MC. SWISS-MODEL and the Swiss-PdbViewer: an environment for comparative protein modeling. *Electrophoresis* 1997;18(15):2714-2723.

[76]Koho T, Huhti L, Blazevic V, Nurminen K, Butcher SJ, Laurinmaki P, et al. Production and characterization of virus-like particles and the P domain protein of GII.4 norovirus. *J Virol Methods* 2012;179(1):1-7.

[77]Bertolotti-Ciarlet A, White LJ, Chen R, Prasad BV, Estes MK. Structural requirements for the assembly of Norwalk virus-like particles. *J Virol* 2002;76(8):4044-4055.

[78]Kolawole AO, Smith HQ, Svoboda SA, Lewis MS, Sherman MB, Lynch GC, et al. Norovirus Escape from Broadly Neutralizing Antibodies Is Limited to Allostery-Like Mechanisms. *mSphere* 2017;2(5):10.1128/mSphere.00334-17. eCollection 2017 Sep-Oct.

[79]Heinimaki S, Tamminen K, Malm M, Vesikari T, Blazevic V. Live baculovirus acts as a strong B and T cell adjuvant for monomeric and oligomeric protein antigens. *Virology* 2017;511:114-122.

[80]Hinrichsen M, Lenz M, Edwards JM, Miller OK, Mochrie SGJ, Swain PS, et al. A new method for post-translationally labeling proteins in live cells for fluorescence imaging and tracking. *Protein Eng Des Sel* 2017;30(12):771-780.

[81]Fierer JO, Veggiani G, Howarth M. SpyLigase peptide-peptide ligation polymerizes affibodies to enhance magnetic cancer cell capture. *Proc Natl Acad Sci U S A* 2014;111(13):E1176-81.

[82]Traynor K. First recombinant flu vaccine approved. *Am J Health Syst Pharm* 2013;70(5):382.

[83]Sutton TC, Chakraborty S, Mallajosyula VVA, Lamirande EW, Ganti K, Bock KW, et al. Protective efficacy of influenza group 2 hemagglutinin stem-fragment immunogen vaccines. *NPJ Vaccines* 2017;2:35-017-0036-2. eCollection 2017.

[84]Lee YT, Ko EJ, Lee Y, Kim KH, Kim MC, Lee YN, et al. Intranasal vaccination with M2e5x virus-like particles induces humoral and cellular immune responses conferring cross-protection against heterosubtypic influenza viruses. *PLoS One* 2018;13(1):e0190868.

10 Appendix: Amino acid sequences of designed proteins

10.1.1 SpyCatcher antigens

SpyCatcher-M2e (His-tag, TEV-site, SpyCatcher, XhoI, M2e, BlpI):

```
MHHHHHHDYD IPTTENLYFQ GSGDSATHIK FSKRDEDGKE LAGATMELRD SSGKTISTWI 60
SDGQVKDFYL YPGKYTFVET AAPDGYEVAT AITFTVNEQG QVTVNGLEMS LLTEVETPIR 120
NEWGCRCNDS SD**                                                   132
```

SpyCatcher-H1F (His-tag, TEV-site, SpyCatcher, XhoI, H1F (Foldon underlined), BlpI):

```
MHHHHHHDYD IPTTENLYFQ GSGDSATHIK FSKRDEDGKE LAGATMELRD SSGKTISTWI 60
SDGQVKDFYL YPGKYTFVET AAPDGYEVAT AITFTVNEQG QVTVNGLEDT VDTVLEKNVT 120
VTHSVNLLED SHGSANSSLP YQNTHPTTNG ESPKYVRSAK LRMVTGLRNG SAGSATQNAI 180
NGITNKVNTV IEKMNIQDTA TGKEFNKDEK RMENLNKKVD DGFLDIWTYN AELLVLLENE 240
RTLDAHDSQG TGGGYIPEAP RDGQAYVRKD GEWVLLSTFL **                    280
```

10.1.2 Monodin antigens

Monodin-M2e (Signal peptide 1, Monodin, XhoI, M2e, BlpI):

```
MIRTNAVAAL VFAVATSALA FDASNFKDFS SIASASSSWQ NQHGSTMIIQ VDSFGNVSGQ 60
YVNRAEGTGC QNSPYPLTGR VNGTFIDFSV KWNNSTENCN SNTQWTGYAQ VNGNNTEIVT 120
RWNLKYEGGS GPAIWQGQDT FQYVPTTELE MSLLTEVETP IRNEWGCRCN DSSD**     174
```

Monodin-H1F (Signal peptide 2, Monodin, XhoI, H1F, BlpI):

```
MKKIWLALAG LVLAFSASAA QDPFDASNFK DFSSIASASS SWQNQHGSTM IIQVDSFGNV 60
SGQYVNRAEG TGCQNSPYPL TGRVNGTFID FSVKWNNSTE NCNSNTQWTG YAQVNGNNTE 120
IVTRWNLKYE GGSGPAIWQG QDTFQYVPTT ELEDTVDTVL EKNVTVTHSV NLLEDSHGSA 180
NSSLPYQNTH PTTNGESPKY VRSAKLRMVT GLRNGSAGSA TQNAINGITN KVNTVIEKMN 240
IQDTATGKEF NKDEKRMENL NKKVDDGFLD IWTYNAELLV LLENERTLDA HDSQGTGGGY 300
IPEAPRDGQA YVRKDGEWVL LSTFL**                                     325
```

10.1.3 Rhizavidin antigens

Rhizavidin-M2e (Signal peptide 1, Rhizavidin, XhoI, M2e, BlpI):

```
MIRTNAVAAL VFAVATSALA FDASNFKDFS SIASASSSWQ NQSGSTMIIQ VDSFGNVSGQ 60
YVNRAQGTGC QNSPYPLTGR VNGTFIAFSV GWNNSTENCN SATGWTGYAQ VNGNNTEIVT 120
SWNLAYEGGS GPAIEQGQDT FQYVPTTELE MSLLTEVETP IRNEWGCRCN DSSD**     174
```

Rhizavidin-H1F (Signal peptide 2, Rhizavidin, XhoI, H1F, BlpI):

```
MKKIWLALAG LVLAFSASAA QDPFDASNFK DFSSIASASS SWQNQSGSTM IIQVDSFGNV 60
SGQYVNRAQG TGCQNSPYPL TGRVNGTFIA FSVGWNNSTE NCNSATGWTG YAQVNGNNTE 120
IVTSWNLAYE GGSGPAIEQG QDTFQYVPTT ELEDTVDTVL EKNVTVTHSV NLLEDSHGSA 180
NSSLPYQNTH PTTNGESPKY VRSAKLRMVT GLRNGSAGSA TQNAINGITN KVNTVIEKMN 240
IQDTATGKEF NKDEKRMENL NKKVDDGFLD IWTYNAELLV LLENERTLDA HDSQGTGGGY 300
IPEAPRDGQA YVRKDGEWVL LSTFL**                                     325
```

10.1.4 Avidin antigens

Avidin-M2e (Signal peptide 3, Avidin, XhoI, M2e, BlpI):

```
MNKPSKFALA LAFAAVTASG VASAQTVARK CSLTGEWTND LGSNMTIGAV NSRGEFTGTY 60
ITAVTATSNE IKESPLHGTQ NTINKRTQPT FGFTVNWKFS ESTTVFTGQC FIDRNGKEVL 120
KTMWLLRSSV NDIGDDWKAT LVGYNIFTRL HTQEELEMSL LTEVETPIRN EWGCRCNDSS 180
D**                                                               181
```

Avidin-H1HA10 (Signal peptide 3, Avidin, XhoI, H1HA10, BlpI):

```
MNKPSKFALA LAFAAVTASG VASAQTVARK CSLTGEWTND LGSNMTIGAV NSRGEFTGTY 60
ITAVTATSNE IKESPLHGTQ NTINKRTQPT FGFTVNWKFS ESTTVFTGQC FIDRNGKEVL 120
KTMWLLRSSV NDIGDDWKAT LVGYNIFTRL HTQEELEDTV DTVLEKNVTV THSVNLLEDS 180
HGSANSSLPY QNTHPTTNGE SPKYVRSAKL RMVTGLRNGS AGSATQNAIN GITNKVNTVI 240
EKMNIQDTAT GKEFNKDEKR MENLNKKVDD GFLDIWTYNA ELLVLLENER TLDAHDS**  297
```